A Novel Remodulation Scheme for WDM PONs Using DPSK for Both Downstream and Upstream

Nebras Deb

A thesis submitted to
The Faculty of Graduate and Postdoctoral studies
in conformity with the requirements for the degree of
Master of Applied Science (M.A.Sc)
degree in Electrical Engineering

Ottawa-Carleton Institute for Electrical and Computer Engineering
School of Information Technology and Engineering
University of Ottawa
Ottawa, Ontario, Canada

uOttawa

Abstract

Wavelength Division Multiplexing Passive Optical Networks (WDM PONs) offer a great solution to satisfy the increasing demand of bandwidth. In addition, it offers a higher level of data security through virtual point to point connections. A great challenge in realizing cost-effective WDM PON is the need for a transmitter at each Optical Network Unit (ONU) with a dedicated wavelength, which overloads the total cost of the system, in addition to reducing the number of available wavelengths in the system. Remodulation scheme is an ultimate solution for these problems of WDM PONs as the downstream signal itself is remodulated with upstream data which saves the need for a laser source at the ONU side.

In this thesis I propose and experimentally demonstrate a novel wavelength remodulation scheme for WDM PONs that employs Differential Phase Shift Keying (DPSK) for downstream and Return to Zero DPSK (RZ-DPSK) for upstream. The use of DPSK enhanced the system with improved receiver sensitivity and RZ-DPSK improved the tolerance toward chromatic dispersion.

In addition, I investigate the Backreflection (BR) penalty resulting from beat noise of BRs with upstream signal in a bidirectional WDM PON system that uses remodulation and phase modulation as a modulation format. I experimentally demonstrate the optimal conditions to operate the system and minimize the BR penalty.

Acknowledgment

First and foremost I would like express my heartfelt gratitude to Dr. Hanan Anis. As a supervisor, it was a great experience to work under her supervision, with her persistent guidance and support throughout my study in the Master's. Dr. Anis did not only teach me research mythology and professional knowledge, but also gave me invaluable suggestions on paper writing and presentation skills. I believe the knowledge and experience I earned under Dr. Anis's supervision will lighten my way in all my future research and work.

I was also very fortunate to be with the lab group members; they have always been there when I needed them in the academic matters or even as dear friends, I wish them all the best for their future and thank them for the good times that made my life in the lab a wonderful experience.

I would like to thank all the individuals in both Ottawa and Carleton University, who gave me support in my research and course work, professors, students, administrative and lab staff.

There is one man that had a great impact on my personality, and inspired me to be more creative, patient, and hardworking. A genius programmer and philosopher, he passed away while I was doing my research, and I believe he has a role in this work, to Sirry's soul I give my blessings.

And last but not least, I would like to thank my beloved parents, brothers and sisters for being supportive and encouraging, and to my parents I dedicate this work.

Table of Contents

List of Figures

Glossary

APDs: Avalanche Photodiodes

ASE: Amplified Spontaneous Emission

AWG: Arrayed Waveguide Grating

B2B: Back-To-Back

BER: Bit-Error-Rate

BERT: Bit Error Rate Test

BPSK: Binary Phase Shift Keying

BLS: Broadband Light Source

BPON: Broadband PON

BR: Backreflection

CD: Chromatic Dispersion

CLS: Centralized Light Sources

CO: Central Office

CW: Continuous Wave

DBR: Distributed Bragg Reflector

DLI: Delay Line Interferometer

DFB: Distributed Feedback Laser

DPSK: Differential Phase Shift Keying

DQPSK: Differential Quadrature Phase Shift Keying

DSFs: Dispersion Shifted Fibers

EAMs: Electro Absorption Modulators

EDFA: Erbium Doped Fiber Amplifier

EPON: Ethernet PON

ER: Extinction Ratio

FMD: Full Modulation Depth

FP: Fabry-Parot

FTTH: Fiber-To-The-Home

GPON: Gigabit PON

IF: Intermediate Frequency

IMDD: Intensity-Modulated/Direct-Detection

ISI: Inter Symbol Interference

LiNbO3: Lithium Niobate

LO: Local Oscillator

LS: Laser Source

MZI: Mach-Zehnder Delay Interferometer

MZM: Mach-Zehnder Modulator

NRZ: Non-Return-To-Zero

ODL: Optical Delay Lines

OLT: Optical Line Terminal

ONT: Optical Network Terminal

ONU: Optical Network Unit

OOK: On-Off Keying

ORL: Optical Return Loss

PLL: Phase-Locked Loop

PONs: Passive Optical Networks

PSK: Phase-Shift Keying

QAM: Quadrature Amplitude Modulation

RIN: Relative Intensity Noise

RMD: Reduced Modulation Depth

RN: Remote Node

RSOAs: Reflective Semiconductor Optical Amplifiers

RZ: Return-To-Zero

SMF: Single Mode Fiber

SNR: Signal-To-Noise Ratio

SOAs: Semiconductor Optical Amplifiers

SPM: Self-Phase Modulation

TDM-PONs: Time Division Multiplexing PONs

TECs: Thermoelectric Coolers

TIA: Trans-Impedance Amplifier

TLL: Transmission Line Loss

VCSELs: Vertical Cavity Surface Emitting Lasers

VOA: Variable Optical Attenuator

WDM-PONs : Wavelength Division Multiplexing Passive Optical Networks

Chapter 1

Objective and Contributions

1.1 Objectives

The continuously increasing demand for higher bandwidth driven by media-rich applications such as movies over the Internet and online 3D games, has driven researchers to focus on high bit rate networks up to the last mile. Wavelength Division Multiplexing Passive Optical Network (WDM-PON) represents an ultimate solution that delivers the highest possible bandwidth to the end user by employing all the bandwidth resources of optical fiber. However, the issue of cost remains a challenging aspect of WDM-PONs that needs to be considered in every proposed solution.

Bidirectional transmission is currently used in WDM-PONs as a means of reducing the system cost. However, this alone is not sufficient and to circumvent the cost issue in WDM-PONs a number of research groups have been investigating remodulation techniques. These techniques use the downstream signal itself as an optical carrier for upstream data which result in a significant reduction in system cost.

Several schemes have been proposed for remodulated WDM-PONs, however only few employed advanced modulation formats taking advantage of their improved receiver sensitivity, and these proposed schemes had different limitations which inspired me to design an efficient system that employs advanced modulation formats in remodulated WDM-PONs.

The objective of this thesis is to propose a new WDM-PONs scheme that employs a remodulation technique using an advanced modulation format that improve the system performance, and to investigate the role of Backreflection (BR) in bidirectional WDM-PONs when using my developed remodulation scheme.

1.2 Contributions

There are two main contributions in this thesis

1. I propose and experimentally demonstrate a novel wavelength remodulation scheme for WDM-PONs that employs Differential Phase Shift Keying (DPSK) for both downstream and upstream. The results that I obtained by experiment demonstrated that the proposed scheme is a competitive candidate for WDM-PONs when compared to other WDM-PON remodulation schemes. My scheme depicts an improved tolerance toward Chromatic Dispersion (CD) as well as improved receiver sensitivity [1].
2. I investigate the issue of BR beat noise in bidirectional transmission when using phase modulation in remodulated WDM-PONs. To the best of my knowledge, this work is the first to explore the penalty induced by BR in this case, and the results I obtained by experiment can help tune a system and minimize the penalty of BR for the best performance [2].

1.3 Thesis Outline

The rest of the thesis is organized as follows:

Chapter 2 gives an overview of Passive Optical Networks (PONs), starting with the concept and then defining Time Division Multiplexing PONs (TDM-PONs) and WDM-PONs, and then focusing on WDM-PONs. I then discuss the main schemes that are used for implementing colorless Optical Network Units (ONUs), and end by an overview of the remodulation scheme as one of these schemes.

Chapter 3 focus on phase modulated systems. I start with an introduction about intensity modulation and phase modulation systems, and then I introduce DPSK and give an overview of the main devices used in DPSK systems, as the Mach-Zehnder Modulator (MZM), the Mach-Zehnder Delay Interferometer (MZI), pulse carvers and the differential precoder for DPSK. I finish the chapter with an overview of different

impairments on the transmission system, emphasizing CD, BR, and Self-Phase Modulation (SPM).

Chapter 4 demonstrates the experimental research that I carried out, starting with the novel remodulation scheme for WDM-PONs that uses DPSK for both downstream and upstream, with a detailed description of the setup, the operation principle, and the experimental results with a discussion. Then I move to the BR experiment, investigate BR in remodulated WDM-PONs when using phase modulation, and I show the results of all my measurements, with a discussion and comparison with the results of On-Off Keying (OOK) [3].

Chapter 5 ends the thesis with a summary and future work that can be developed starting from the work in this thesis.

Publications

1. Nebras Deb and Hanan Anis, "Wavelength remodulation scheme using DPSK downstream and upstream for DWDM-PONs," Opt. Express 19, 16418-16422 (2011).
2. Nebras Deb, Shiyu Gao, and Hanan Anis, "Impact of backreflections on bidirectional WDM-PONs with wavelength remodulation schemes" (To be submitted).

Chapter 2

Passive Optical Networks

The access network, also known as the "first-mile network," connects the service provider to businesses and residential subscribers. This network is sometimes referred to as the subscriber access network. The bandwidth demand in the access network has been increasing rapidly over the last few years, as subscribers are demanding first-mile access solutions that have high bandwidth and offer media-rich services. PONs have evolved to satisfy this increasing demand for bandwidth.

PONs have the feature of having only passive components between the Central Office (CO) and the end user. So they do not contain regenerators, amplifiers, switches or any other active power-consuming elements throughout the whole optical network. Hence PONs have lower cost, are easier to maintain and are more reliable when compared to active Fiber-To-The-Home (FTTH) systems.

Standard PON networks have tree topologies, and this allows the sharing of the cost of fiber deployments in comparison with a point-to-point topology. In a PON scheme, I define the equipment that resides at the CO as the Optical Line Terminal (OLT), while the one residing at the customer's side is known as the ONU. In this chapter, I shall provide an overview of PON's various technologies focusing on WDM-PONs'.

2.1 Time Division Multiplexed PONs

The most common architecture of PONs is TDM-PONs, where two optical wavelengths are used for transmission, one in each direction as I show in Figure 2.1. In the downstream direction the system works in a broadcast mode as the same data is being transmitted from the OLT to all ONUs through the fiber and the Remote Node (RN), and then each ONU identifies and retrieves only the information that is intended for it. In the upstream direction, the upstream data from all ONUs are coupled together into the fiber back to the OLT, one should note that splitting the signals at the RN causes loss.

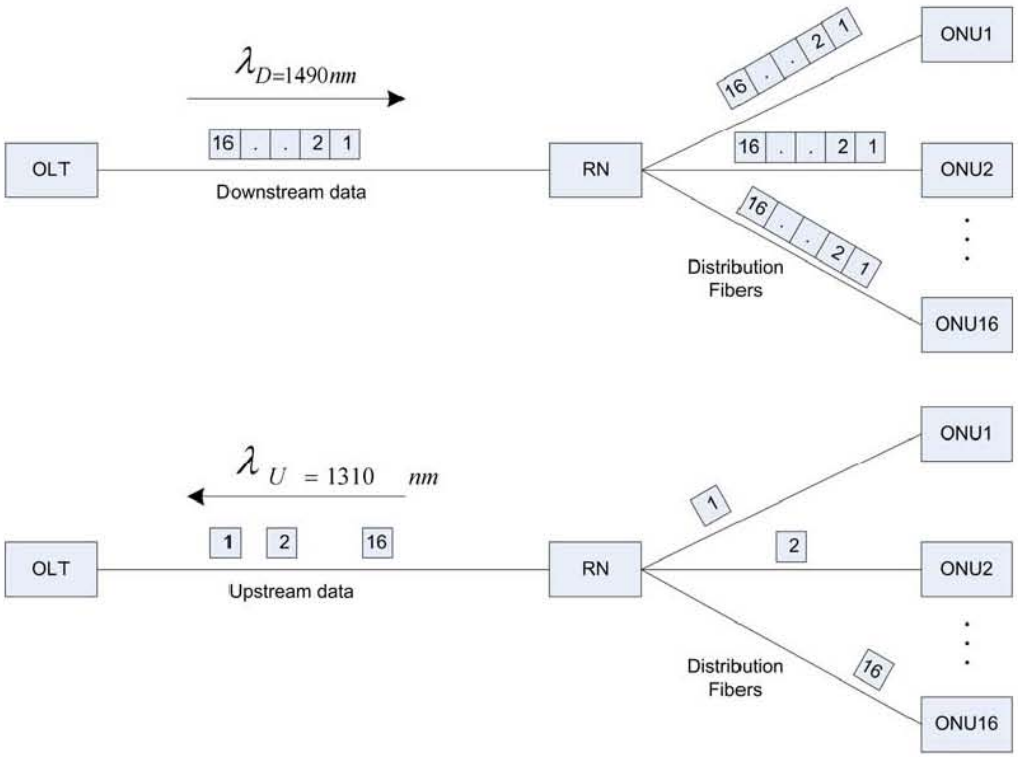

Figure 2.1: Time Division Multiplexed Passive Optical Networks.

One should notice that even though every ONU receives the same signal, the received power varies according to the distance to the particular ONU; i.e. further ONUs

receive less power than closer ones, because the attenuation the signal suffers is proportional to the distance it travels through the fiber.

The signals coming upstream from all ONUs are coupled in the RN and then sent through the fiber to the OLT, and because the RN is a passive device, it's possible that two signals collide in the fiber; therefore the OLT performs scheduling between them, and assigns time slots for the different ONUs. And without that it would be impossible for the OLT to read the upstream signals from different ONUs.

Having the downstream signal working in a broadcast mode helps reduce the cost of electrical receivers at the ONUs, because the downstream signals are transmitted in a continuous mode, so there is no need for re-synchronization, while in the upstream direction the signals are sent in a burst mode, which requires the use of fast burst-mode receiver at the OLT which is more expensive than the receivers at the ONUs. However the cost of this receiver is shared among all users.

There are three different TDM-PON standards, which I compare in Table 2.1. These are Broadband PON (BPON), Ethernet PON (EPON) and Gigabit PON (GPON).

Table 2.1: TDM-PON Standards

	EPON	BPON	GPON
Standards	IEEE 802.3ah	ITU G.983	ITU G.984
Framing	Ethernet	ATM	GEM / ATM
Maximum Downstream Bandwidth	1.25 Gbit/s	622 Mbit/s	2.5 Gbit/s
Maximum Upstream Bandwidth	1.25 Gbit/s	622 Mbit/s	1.25 Gbit/s
Typical Users per PON	32	32	32 / 64
Avg Downstream Bandwidth / User	30 Mbit/s	20 Mbit/s	80 Mbit/s

Typical PON Reach	20 km	20 km	20 km
ODN Loss Budget	28 dB	28 dB	28 dB

2.2 Wavelength Division Multiplexed PONs

The main goal of WDM-PONs is providing much higher bandwidth per user compared to other PONs configurations. In WDM-PONs, the capacity of the network is much higher than that in TDM-PONs.

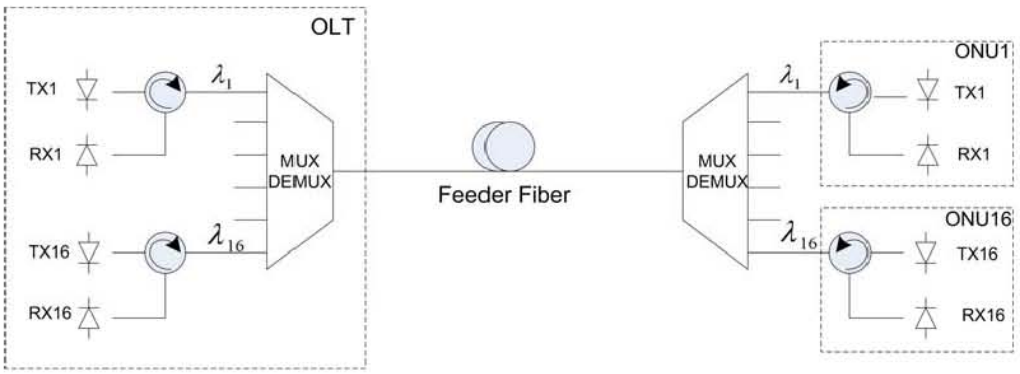

Figure 2.2: Basic model of WDM-PON

Figure 2.2 shows an example of a basic WDM-PON. The OLT contains a group of transmitter-receiver pairs, each pair operates at a certain wavelength λ_n that is specified for a certain user, and this pair is connected to a passive multiplexing device like an Arrayed Waveguide Grating (AWG). The AWG at the OLT connects to another AWG at the distribution network through a Single Mode Fiber (SMF), and this other AWG has an ONU connected to each of its ports. Each ONU contains a pair of transmitter-receiver that also operates at a certain wavelength. The distribution network can include several AWGs cascaded to increase flexibility as in [1], however every AWG in the network will cause additional loss to both downstream and upstream signals.

One of the main issues of such a basic scheme described in Fig. 2.2 is having a laser source at each ONU, Which results in two main practical problems, first is an

increased cost of the ONU, second is an inventory problem because each ONU will need to be customized, and the service provider has to keep an inventory of multiple types of replacement ONUs in stock for the users. Therefore it is necessary to have cost-effective implementations of light sources at the ONU side and also the ONUs need to be colorless (wavelength-independent) to avoid the inventory problem.

Several schemes have been proposed for the implementation of colorless ONUs in WDM-PONs, by the use of spectral sliced Broadband Light Source (BLS), injection locked Fabry-Parot (FP) lasers, or remodulation of downstream signal at the ONU that is based on MZMs, Reflective Semiconductor Optical Amplifiers (RSOAs) or Semiconductor Optical Amplifiers (SOAs). In the following sections, I discuss some of the most important enabling technologies for WDM-PON and the resulting network architectures.

2.2.1 WDM-PONs based on Spectral Slicing

Another solution for solving the inventory problem of laser sources at the ONU is using a BLS and slicing its spectrum, such as a super-luminescent light emitting diode [4], Erbium-Doped Fiber Amplifier (EDFA) [5] or FP laser [6]. The selection of wavelength could be done at the AWG that is located at the RN, as it slices a narrow spectrum of the broadband optical signals, and this would eventually select a different wavelength for each ONU. This technique was first used for downstream transmission [7], and later for upstream [4, 8, 9]. Figure 2.3 shows the principle of this technique when using it for upstream transmission.

In each ONU there is a BLS that is modulated with upstream data. The AWG slices the spectrum of each ONU, and then all the upstream sliced signals are multiplexed

on the fiber until they reach the OLT, then they are demultiplexed and each signal is detected by a separate receiver.

The BLS spectrum should be wide enough to cover all the band of the AWG, and the output power should be high as it would suffer several power losses, starting with the slicing process which leads to significant power loss, e.g. 10 dB [8], and then the loses along the feeder fiber (20km in the standard case), in addition to the coupling, connectors and devices losses.

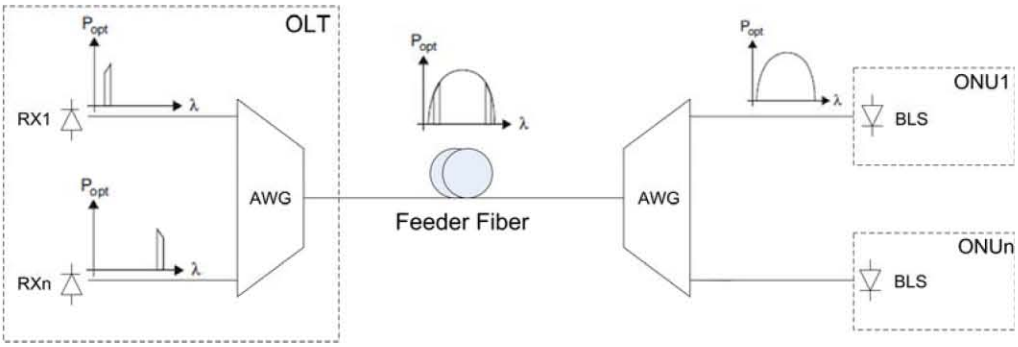

Figure 2.3: Broadband Light Sources WDM-PON

One issue with the spectral slicing technique is the thermal sensitivity of the AWG, as these devices are usually located in the outside plant; therefore it is important that temperature changes do not affect their wavelength properties or else they cause adjacent-channel crosstalk, which has been proven to be the major problem of this technique [9].

The spectral slicing technique has several advantages, such as simple implementation, low cost, and identical ONUs, while it suffers several disadvantages like limited modulation speed, and low power.

When compared to some TDM-PONs deployments that have more than one splitting point, spectral slicing technique has lower flexibility in the network topology, because the signals need to be sliced at the AWG before combining them.

2.2.2 WDM-PON Based on Injection-Locking

In this technique a multiple-longitudinal-mode laser such as a FP laser is injected by an external narrow band optical signal, and this injection locks the lasing mode of the laser to a single mode. The injected optical signal works as a seed for laser oscillation, and the mode that is closest to the injected wavelength is locked to it, while other modes are suppressed [10]. The seed signal can be a spectral sliced broadband source [11], or even the modulated downstream signal itself [12].

The technique of FP injection locking has the advantages of low cost and simplicity, with a relatively high modulation speed, while the disadvantages are limited wavelength locking range, stability, and the requirement for high power. To improve the efficiency of FP injection locking, one should carefully choose the laser bias current, modulation index, and the power of the injected signal [13].

Several architectures were proposed for WDM-PONs based on injection locking [14, 5]. One example is shown in Figure 2.4, where injection locking was employed in both the downstream and upstream [5]. A BLS located at the OLT generates a broad band signal that is sent downstream to the ONUs after slicing it through the remote AWG, and is used for injection-locking of all ONUs' FPs.

In each ONU, a locked FP laser is modulated and the data is sent in the upstream signal back to the OLT where it is circulated and detected by a designated receiver.

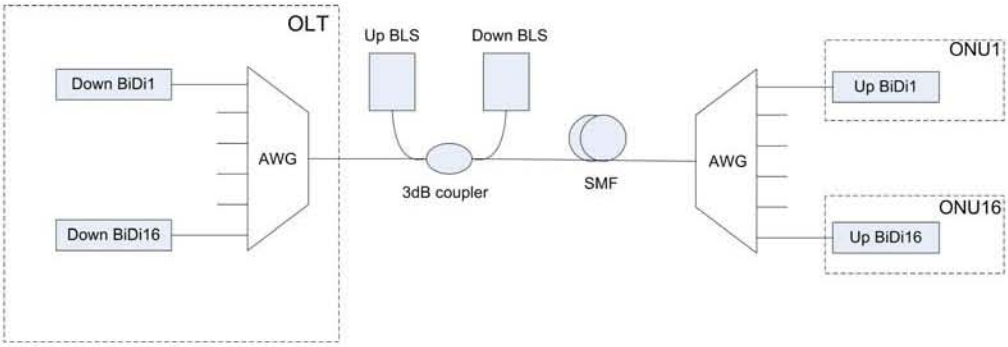

Figure 2.4: Injection locked FP laser WDM-PON.

In this architecture, one should carefully choose the optical injected power, as it needs to be high to achieve high data rates, but in the same time BR limits the level of power we can operate, as the signal is transmitted bidirectionally on the same wavelength of the injected signal [5].

2.2.3 WDM-PON Based on Remodulation

This technique is used to achieve colorless ONUs by the use of Centralized Light Sources (CLS) at the OLT, as Figure 2.8 shows the optical signal coming from the OLT is remodulated with the upstream data and then sent back to the OLT, therefore the ONU does not contain any light source at all, and hence there is no need for wavelength assignment protocol in the optical network.

Several schemes for remodulation have been proposed, including the use of MZMs at the ONU for upstream data modulation, or the use of SOAs or RSOAs. Both SOAs and RSOAs have the advantage of modulating and amplifying the signal in the same time, which saves the cost of having an amplifier in the ONU.

On the other hand, several data modulation schemes have been proposed to achieve bidirectional transmission in the remodulation technique, and these include OOK-OOK using different values of power offset, OOK-DPSK, and DPSK-OOK. In this thesis I propose a novel remodulation system using DPSK-DPSK with an external phase modulator at the ONU as I will explain later in chapter 4. The different schemes vary in their capabilities and limitations [15, 16, 17, 18].

One main disadvantage of the remodulation technique comes from using the same wavelength in both the directions of downstream and upstream, as this result in beating noise between BRs and the main signals. To address this issue I studied the effect of BR in remodulation and especially in my proposed remodulation scheme as we will see later in this thesis (chapter 4).

Another disadvantage of this technique is the polarization sensitivity of the RSOAs or optical modulators. Therefore extensive research is being carried out in the last few years to develop polarization insensitive RSOAs t.

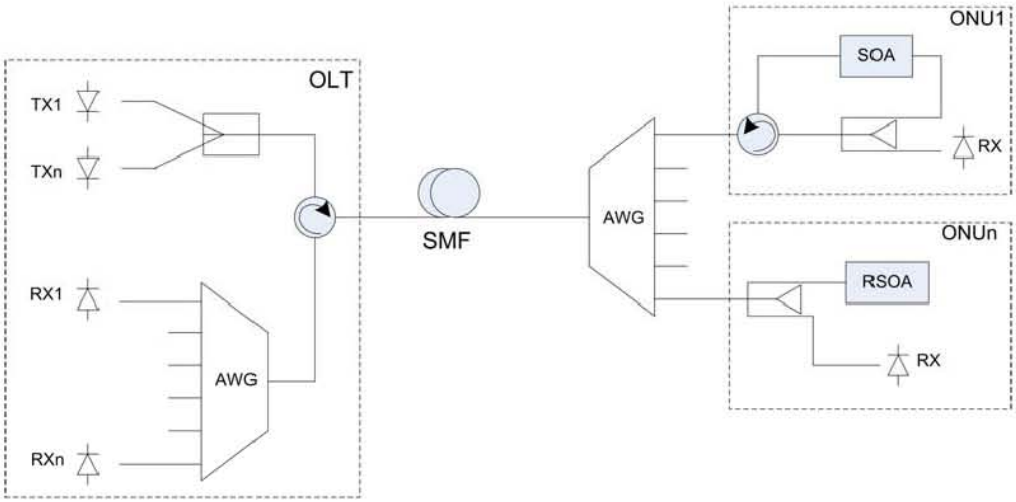

Figure 2.5: Centralized Light Sources WDM-PON.

In addition to the polarization sensitivity, RSOAs also have the problem of temperature sensitivity, so they require Thermoelectric Coolers (TECs) in the same package; therefore manufacturers are working on developing RSOAs that do not require TEC control mechanism by using new materials [19]. This will result in reducing the relatively high cost of RSOAs for access networks.

Figure 2.5 shows an illustration of a generic CLS architecture, as we can notice all light sources are located in the OLT, where they generate the optical power that is used to carry downstream data and also to be a signal that is later modulated in the ONU to produce upstream signal. A passive circulator at the OLT directs the received upstream signals to an array of designated receivers for all users. The optical power should be high enough for the signal to travel down and then upstream, and at the same time it is limited by the effect of BR that is proportional to the optical power.

As I mentioned before, this kind of PONs based on WDM-PON with remodulation is the main subject of my experimental work in this thesis and specifically using phase modulation as a modulation format for both downstream and upstream.

Chapter 3

Phase-Modulated Systems

3.1 Intensity-Modulated Systems

In the past, most fiber optic communication systems used the simple intensity modulation which is also called OOK or Intensity-Modulated/Direct-Detection (IMDD). In this type of modulation, data is carried in the intensity of light, and restored at the receiver side using a photodiode.

Figure 3.1 shows a typical externally modulated IMDD system, where a laser diode at the transmitter side generates the optical carrier which is launched into an intensity modulator, and the modulator acts like a fast switch which turns on-off to represent the data that is intended for transmission, after that the modulated light signal is launched into the fiber which delivers the signal to the receiver.

At the receiver side, a fast photodiode converts the optical signal into electrical one i.e., from optical intensity into electrical current i(t). After the photodiode, a Trans-Impedance Amplifier (TIA) converts the current into voltage that represents the received signal, which is the same as the electrical transmitted signal (data) but with some noise.

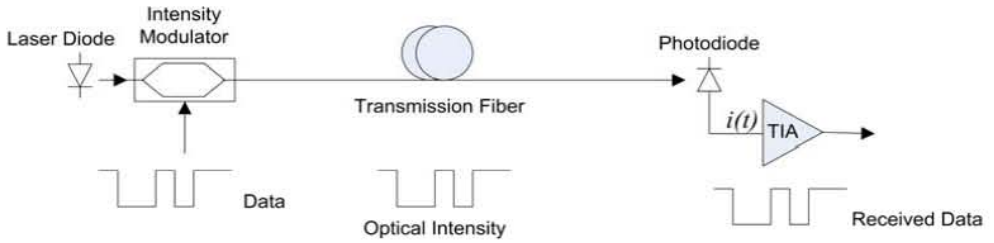

Figure 3.1. Typical configuration of an intensity-modulated/direct-detection (IMDD) system.

Such a system as shown is Fig. 3.1 is straight forward, as the receiver decides the logic of the received data based on the presence or absence of light, and today most of optical communication systems use this principle, with different formats, as Non-Return-To-Zero (NRZ) or Return-To-Zero (RZ) pulses for transmission.

In many applications the laser diode at the transmitter could be directly modulated which saves the need for an external modulator; however this affects the signal quality. Moreover, in some low speed applications a simple light-emitting diode could be used as a light source with multimode fibers. In these applications the need for alignment between the fiber and the light source is reduced significantly because of the large core of a multimode fiber.

3.2 Phase-Modulated Systems

The principle of carrying data in the phase of the carrier is used in most digital communication systems [20] both in wireless or wireline transmission.

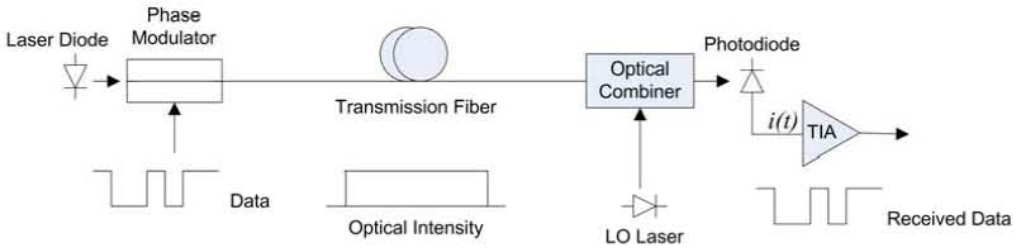

Figure 3.2. Basic scheme of phase-modulated optical communication system.

Figure 3.2 shows a basic scheme of a phase-modulated optical communication system based on Phase-Shift Keying (PSK). At the transmitter side, the optical carrier is generated by a laser diode, and then passed through a phase modulator, which writes the data on the phase of the optical signal. The signal is launched into the transmission fiber to the receiver. In the receiver the phase modulated signal is mixed with the light of a Local Oscillator (LO) laser, and this process converts the signal frequency from the original value in THz to the range of GHz (microwave frequency), as this mixing process generates a beating signal at the photodiode which its frequency is an Intermediate Frequency (IF) equals the difference between the two optical signals of the LO and the received one.

In the special case where the frequency of the LO laser is the same as the carrier frequency of the received signal the system is called a homodyne system, while in the general case when the two frequencies are different it is called a heterodyne system with an IF of

$$\omega_{IF} = \omega_c - \omega_{LO} \qquad (3.1)$$

Where ω_c, and ω_{LO} are the frequency of the transmitted signal and LO laser, respectively. In homodyne systems, $\omega_{IF} = 0$.

If we compare the two systems in Fig. 3.1 and Fig 3.2 we notice that in the IMDD system the intensity of the signal varies along the fiber depending on the data, while in the PSK system the intensity does not depend on the data, as the data is carried in the phase of that signal, however this changes after the demodulator, as the optical combiner (demodulator) in Fig 3.2 works as a converter from the phase domain to the amplitude domain by mixing the optical signal with the signal of LO laser.

In digital communications [20], a coherent system always requires carrier recovery, and this translates to phase locking in homodyne systems, while in heterodyne systems the carrier recovery is conducted in the IF signal of ω_{IF}. In coherent optical communication systems a different terminology is used than digital communications, as an optical system is called "coherent" based on having mixing of optical signals

even without carrier recovery, therefore even a DPSK system is considered as a coherent optical system [21].

The use of coherent systems goes back to the earliest date of optical communications [22], and it was firstly used in free space by mixing high power lights; coherent systems are still used today for inter-satellite communications [23].
In both coherent and phase-modulated optical communications, it is very important to reduce the frequency and phase noise of the laser source. In other words, the laser source must be highly coherent in phase modulated systems, because this kind of noise adds directly to the phase or frequency of the optical carrier, while in IMDD systems the coherence of the source does not seriously affect the performance of the system.

Optical coherent communications attracted a lot of attention in the 80's [24], [25], [26]. This is due to their advantage in improving the receiver sensitivity and significantly improving the range of transmission that can be achieved, as beating the signal with a LO laser signal plays the roll of amplification, and achieves up to 20 dB better receiver sensitivity when compared with the IMDD systems. The interest in coherent systems somewhat decreased with the appearance of EDFAs [27] as it presented a cheaper and more practical solution to improving receiver sensitivity.
However, direct detection has generated a lot of interest in the last decade [28] due to its simplicity and lower cost when compared to coherent detection. Using DPSK in WDM-PONs seems like a natural extension particularly due to their increased receiver sensitivity when compared with OOK.
In the following sections, I will give an overview about the principles of PSK and DPSK systems as examples of optical phase modulated systems.

3.2.1 PSK Systems

In optical PSK systems data is carried in the phase of the optical carrier, as shown in Fig 3.2 the transmitter of a PSK system consists of a laser diode followed by a phase modulator that is driven by an electrical amplifier of the electrical signal representing data to be transmitted. The phase modulator applies a certain phase shift to the Continuous Wave (CW) carrier (in binary PSK the modulator applies a phase shift of 0^{o} or 180^{o}).

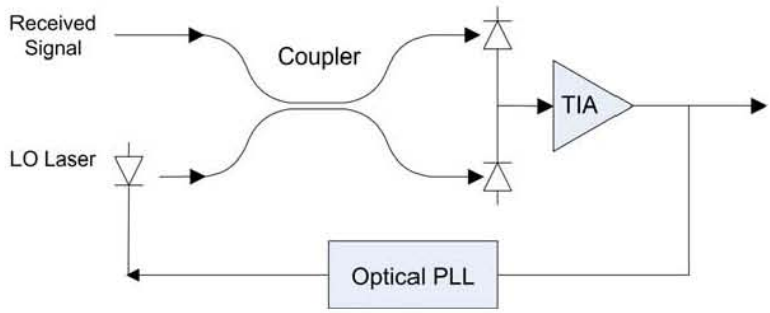

(a) Homodyne PSK receiver

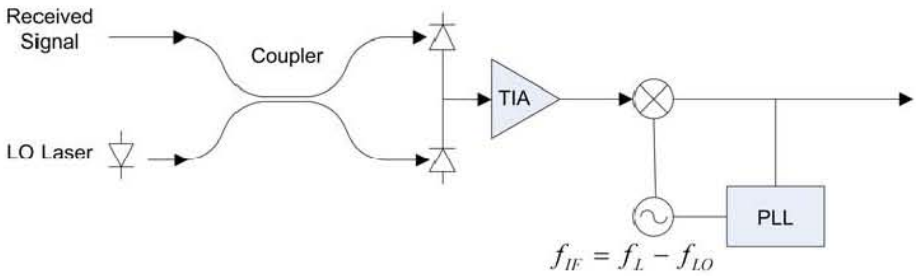

(b) Heterodyne PSK receiver

Figure 3.3. Schematic structure of homodyne and heterodyne PSK receiver.

An optical PSK signal could be detected by either a homodyne or heterodyne receiver as shown in Fig 3.3. In homodyne receivers the LO frequency must be the same as the transmitter laser, and also it must be coherent in phase with it, therefore an optical Phase-Locked Loop (PLL) is used to lock the phase of the LO to that of the transmitter laser. The optical coupler in Fig 3.3 work as 90° optical hybrid, so its outputs have 180° phase difference (I will provide more details about couplers later in this chapter).

In heterodyne receivers, the received signal is mixed with the signal of LO laser, and the beating between them generates an IF signal, and for this to be fixed, frequency locking is required. In addition to that, the recovery of the transmitted phase requires the use of an electrical PLL that operates at ω_{IF}.

In both the receivers of Fig. 3.3, a balanced receiver is used instead of a single photodiode, and it offers several advantages as it maximizes the signal power and

suppresses the intensity noise of the LO [29]. One issue in PSK receivers is adjusting the polarization of the LO laser to be the same as the polarization of the transmitter.

Even though they offer high receiver sensitivity, due to the requirement of an optical PLL, and the general difficulty in designing PSK receivers, the interest in optical PSK systems in research was limited particularly with the introduction of EDFAs. However, the recent advancement of technology is helping to overcome these challenges, and therefore bringing coherent systems again to the forefront of research.

3.2.2 DPSK Systems

In optical DPSK systems, data is carried in the phase difference of an optical carrier between two successive bits. As shown in Fig 3.4 the transmitter of DPSK is the same as the transmitter of PSK shown in Fig 3.2 except the need for an electrical precoder that modifies the driving signal of the phase modulator, and this precoder at the transmitter side saves the need for a decoder circuitry at the receiver of DPSK. Further details about the structure of differential precoder are given later in this chapter.

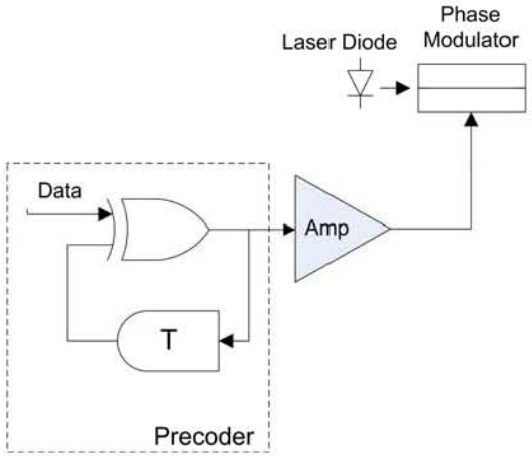

(a) DPSK transmitter

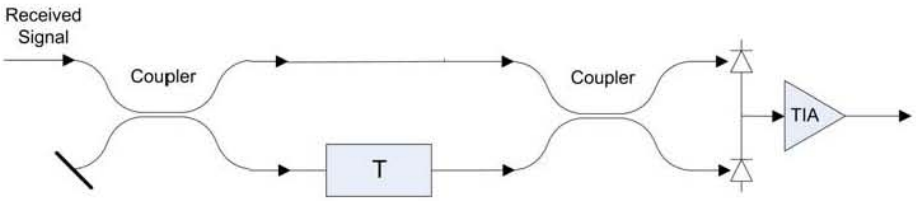

(b) Direct-Detection DPSK receiver

Figure 3.4. Transmitter and receiver for optical DPSK

A DPSK signal can be detected by a direct-detection DPSK receiver as shown in Fig. 3.4, it consists of an interferometer that splits the received signal to two paths, delays one of them by 1 bit time, and then recombines them together, and this translates to mixing the received signal with a delayed version of itself instead of mixing it with a LO signal in PSK systems. Several configurations of heterodyne receivers could also be used to detect DPSK, however without any advantage in performance on the direct detection receiver [30], [31]. When comparing with IMDD systems, we find that the direct detection receiver of DPSK is more complicated, however it is far simpler than the coherent receiver with a LO laser.

In the following section, I will discuss the devices that are used in phase-modulated systems, and provide the basic mathematical formulas that identify them. In addition, I will explain DPSK in more detail given that I used DPSK in all my experiments.

3.3 Optical phase modulator and demodulator

In phase-modulated systems, MZM and MZI are basic components used at the transmitter and receiver side respectively. In the following, I give conceptual model of them.

3.3.1 Optical Lithium Niobate Modulator

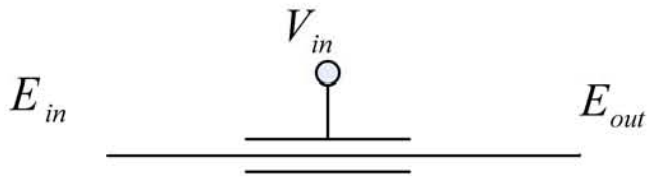

Figure 3.5. Optical Lithium Niobate modulator.

Figure 3.5 shows a scheme of the structure of an optical Lithium Niobate ($LiNbO_3$) modulator. It is an optical device which incorporates light in the $LiNbO_3$crystal with higher refractive index than the surrounding medium, and based on electro-optic effect the refractive index of $LiNbO_3$ crystal can be changed by applying a voltage V_{in} which results in changing the phase of the passing signal.

If E_{in} is the electric field of the input signal and E_{out} is the electric field of the output signal, then

$$E_{out} = e^{j\theta} E_{in} \qquad (3.2)$$

The function of phase shift versus applied voltage is assumed to be linear:

$\theta = \pi\left(\frac{V_{in}}{V_{\pi}}\right)$, where V_{π} is the input voltage that adds (180°) phase shift to the optical signal. This model is a good approximation for phase modulators based on the electro-optic effect in $LiNbO_3$ devices [32].

Practically, $LiNbO_3$ phase modulators suffer from transient chirp. Moreover the imperfections in the driving waveform get directly mapped to the optical phase thus potentially degrading performance [33].

In contrast, as we will show in section 3.3.3, LiNbo3 MZM is robust toward variations in drive level when used for phase modulation. a good comparison between the use of phase modulator and MZM for phase modulation could be found in [33].

3.3.2 Optical Coupler

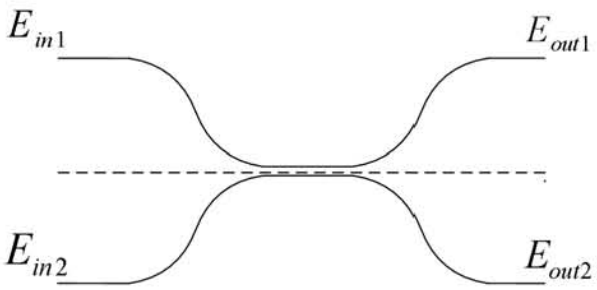

Figure 3.6. Optical coupler.

Figure 3.6 shows a schematic structure of an optical coupler. When neglecting the backward going waves, then the action of a fiber coupler is governed by the matrix equation of $E_{out} = TE_{in}$, where T is the 2 x 2 transfer matrix and E is a column vector of which two components represent the input (or the output) optical fields at

the two ports. For a lossless coupler and when neglecting the backward going waves, the transfer matrix T should be both symmetric and unitary, the symmetric requirement results from time reversal property of light, and the unitary property holds for a lossless coupler. Thus the most general form of this matrix is $T=\begin{pmatrix} a & b \\ b & a \end{pmatrix}$, with the property of $a^2-b^2=1$. At the same time, $|a^2|+|b^2|=1$ is imposed because the total power does not change during splitting. We can take a to be real. Then, these two requirements are met only if $a=\sqrt{\psi}$ and $b=j\sqrt{1-\psi}$ then we can write

$$\begin{pmatrix} E_{out1} \\ E_{out2} \end{pmatrix}=\begin{pmatrix} \sqrt{\psi} & j\sqrt{1-\psi} \\ j\sqrt{1-\psi} & \sqrt{\psi} \end{pmatrix}\begin{pmatrix} E_{in1} \\ E_{in2} \end{pmatrix} \qquad (3.3)$$

For an ideal case $|a|=|b|=\sqrt{1/2}$, that means the power of both output arms is equal. This kind of coupler is usually used as a power splitter, and it is also called 3dB coupler. We can write the matrix of a 3dB coupler as

$$\begin{pmatrix} E_{out1} \\ E_{out2} \end{pmatrix}=\frac{1}{\sqrt{2}}\begin{pmatrix} 1 & j \\ j & 1 \end{pmatrix}\begin{pmatrix} E_{in1} \\ E_{in2} \end{pmatrix} \qquad (3.4)$$

3.3.3 Optical Mach-Zehnder Modulator

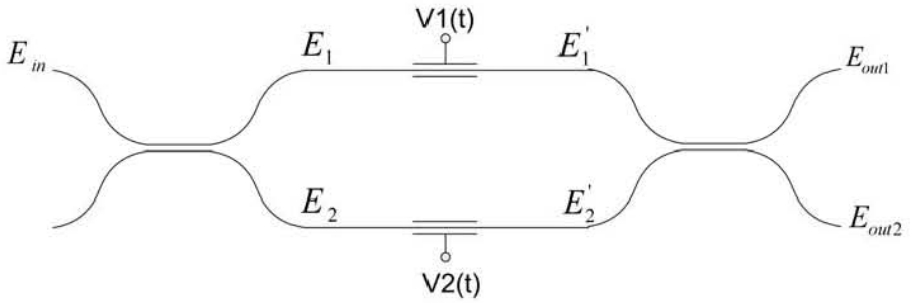

Figure 3.7. Optical Mach-Zehnder modulator.

Figure 3.7 shows a scheme of dual arm optical MZM. E_{in} is the electric field of the input optical signal, and E_1 and E_2 are the outputs of the first optical coupler. $V_1(t)$ and $V_2(t)$ are the driving voltages of two $LiNbO_3$phase modulators. E_1' and E_2' are

the output optical signals of two phase modulators. E_{out1} and E_{out2} are the outputs of the MZM.

A dual-arm MZM is constructed by connecting two 3dB optical couplers using two $LiNbO_3$phase modulators in parallel. The first coupler works as a power splitter as it splits the input signal into two signals of the same power. Before applying any external voltage on the two arms, the optical signals in the two arms of the MZM experience identical phase shifts and interfere constructively and destructively at the two outputs of the second coupler. When a voltage is applied to either one of the two arms, an additional phase shift is introduced which changes the state of interference.

The electric field of the input optical signal is represented as $E_{in} = |E_o| e^{j\omega_c t}$ where $|E_o|$ is optical electric field amplitude; ω_c is radian frequency of optical carrier. In this instance we consider the exponential representation of the time varying part of the optical electric field. The first 3dB coupler splits E_{in} into E_1 and E_2

$$\begin{pmatrix} E_1 \\ E_2 \end{pmatrix} = \frac{1}{\sqrt{2}} \begin{pmatrix} 1 & j \\ j & 1 \end{pmatrix} \begin{pmatrix} E_{in} \\ 0 \end{pmatrix} \tag{3.5}$$

Consider the transfer function of an ideal $LiNbO_3$phase modulator, $E_1^{`} = E_1 e^{j\theta_1}$ and $E_2^{`} = E_2 e^{j\theta 2}$. The second 3dB coupler combines $E_1^{`}$ and $E_2^{`}$, and E_{out1} and E_{out2} are given by:

$$\begin{pmatrix} E_{out1} \\ E_{out2} \end{pmatrix} = \frac{1}{\sqrt{2}} \begin{pmatrix} 1 & j \\ j & 1 \end{pmatrix} \begin{pmatrix} E_1^{`} \\ E_2^{`} \end{pmatrix} \tag{3.6}$$

After calculation we have

$$E_{out1} = 0.5E_{in} e^{j\theta_1} - 0.5E_{in} e^{j\theta_2} = jE_{in} \sin\frac{\theta_1 - \theta_2}{2} \exp\left(j\frac{\theta_1 + \theta_2}{2} \right) \tag{3.7a}$$

$$E_{out2} = j0.5E_{in}e^{j\theta_1} + j0.5E_{in}e^{j\theta_2} = E_{in}\cos\frac{\theta_1-\theta_2}{2}\exp\left(j\frac{\theta_1+\theta_2}{2}\right) \quad (3.7b)$$

E_{out1} and E_{out2} in equation (3.7) show that MZM can be used either as an amplitude modulator or a phase modulator. When the two arms of the MZM are push-pull driven, that is $\theta = \theta_1 = -\theta_2$ we obtain $E_{out1} = jE_{in}\sin(\theta)$ and $E_{out2} = E_{in}\cos(\theta)$, that is amplitude modulation. Sometimes $E_{out1} = jE_{in}\sin(\theta)$ is called the sine arm and $E_{out2} = E_{in}\cos(\theta)$ is called cosine arm. When the two arms of the MZM have equal electronic driving voltage, that is $\theta = \theta_1 = \theta_2$, we have $E_{out1} = 0$ and $E_{out2} = E_{in}\exp(j\theta)$. We can see that the cosine arm has the same optical power as the input except θ phase shift, and the other arm has no power.

3.3.4 Optical Pulse Carvers (RZ-Modulators)

In optical transmission systems, the shape of optical pulses affects the performance of transmission significantly, and the most common shape used in today's commercial systems is NRZ, in which the "non-zero" bit has power covering the entire bit slot. Another option for pulse shape is the RZ, in which the optical power always goes to zero within each bit period. RZ modulation formats are known to be more robust to propagation penalties as it results in less inter-symbol interference. Moreover nonlinear effects may be reduced through pre-chirp [34].

RZ pulses can be produced either in the electrical domain by electronically generating RZ waveforms, or in the optical domain by carving NRZ pulses using an optical pulse carver. Fig 3.8 shows the structure of an RZ-DPSK transmitter using an intensity modulator which plays the role of a pulse carver, followed by a phase modulator. The intensity modulator is responsible for generating the RZ pulses and should be driven by a sinusoidal signal synchronized with the data source, while the phase modulator writes phase information on the RZ signal and is driven by the precoded data [33].

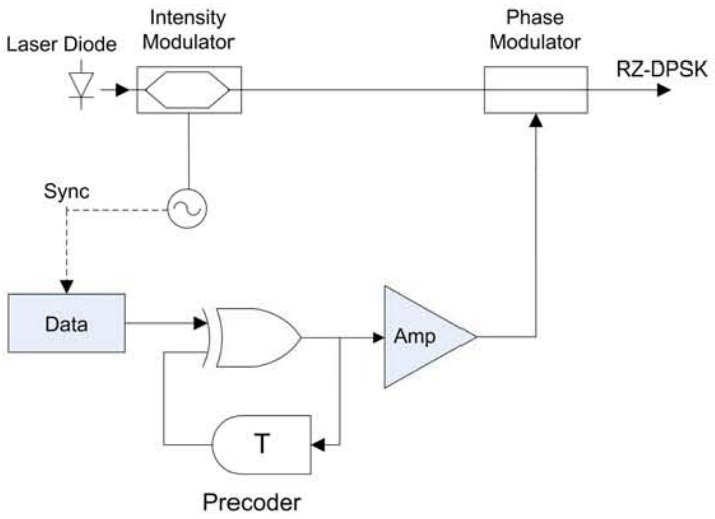

Figure 3.8. Schematic of RZ-DPSK transmitter.

Practically the intensity modulator of the pulse carver would be implemented by an MZM driven in push-pull mode by a sine wave voltage as shown in Fig. 3.9, $V_1 = -V_2 = U\sin(\omega_p t)$ where ω_p is the frequency of the sine wave.

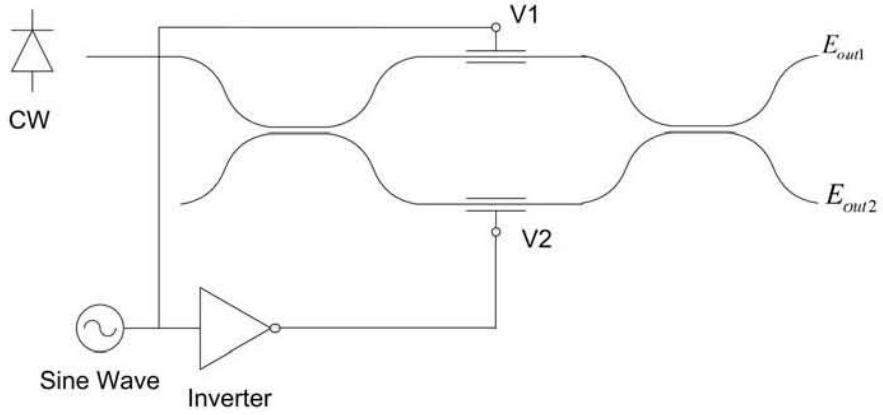

Figure 3.9. Schematic of optical pulse carver.

By using equation (3.7b), and given that $\theta = \pi\left(\frac{V_{in}}{V_\pi}\right)$ we get:

$$E_{out2} = E_{in}\cos\pi\frac{V_1 - V_2}{2V_\pi}\exp\left(j\pi\frac{V_1 + V_2}{2V_\pi}\right) \qquad (3.8)$$

As $V = V_1 = -V_2 = U\sin(\omega_p t)$ then we find

$$E_{out2} = E_{in} \cos \pi \frac{V}{V_\pi} \qquad (3.9)$$

Usually a biasing DC voltage is added to the two phase modulated arms of the MZM to control the duty cycle of the RZ pulses and this is represented with the phase ϕ in the following equation

$$E_{out2} = E_{in} \cos(\pi \frac{V}{V_\pi} + \phi) \qquad (3.10)$$

To generate 50% duty cycle pulses we choose U to equal $U = \frac{V_\pi}{4}$ and $\phi = \frac{\pi}{4}$ such that the maximum drive voltage equals V_π [35].

To generate 33% duty cycle pulses we choose $U = \frac{V_\pi}{2}$ and $\phi = \pi$ such that the maximum drive voltage equals $2V_\pi$.

To generate 66% duty cycle pulses we also choose $U = \frac{V_\pi}{2}$ but $\phi = \frac{\pi}{2}$ such that the maximum drive voltage equals $2V_\pi$.

3.3.5 Optical Mach-Zehnder delay interferometer

At the receiver side of an optical phase transmission system, a photo detector operates on the principle of squared law detection; therefore it is insensitive to phase changes. Consequently, there is a need to convert phase changes into intensity changes that a photo diode can detect and recover the original data that was transmitted through the system. We use a delay interferometer for this specific purpose.

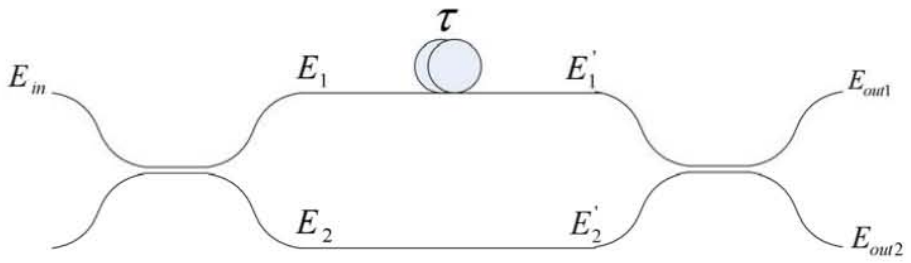

Figure 3.10. Optical Mach-Zehnder delay interferometer.

Figure 3.10 shows a schematic of all fiber MZI. E_{in} is the electric field of the received optical signal. E_1 and E_2 are outputs of first optical coupler. τ is time delay

interval produced by a roll of fiber that equals one bit period. $E_1^{`}$ is the output of the delay line, $E_2^{`} = E_2$, and E_{out1} , E_{out2} are the outputs of the MZI.

An all fiber MZI is constructed by connecting two fiber couplers in series with a delay line on one arm. The first coupler splits the received signal into two equal parts with electric fields E_1 and E_2 :

$$\begin{pmatrix} E_1 \\ E_2 \end{pmatrix} = \frac{1}{\sqrt{2}} \begin{pmatrix} 1 & j \\ j & 1 \end{pmatrix} \begin{pmatrix} E_{in} \\ 0 \end{pmatrix} \tag{3.11}$$

$E_1^{`}$ is the delayed version of $E_1$ therefore $E_1^{`} = E_1(t-\tau)$. The second coupler combines $E_1^{`}$ and $E_2^{`}$, then E_{out1} and E_{out2} are given by

$$\begin{pmatrix} E_{out1} \\ E_{out2} \end{pmatrix} = \frac{1}{\sqrt{2}} \begin{pmatrix} 1 & j \\ j & 1 \end{pmatrix} \begin{pmatrix} E_1^{`} \\ E_2^{`} \end{pmatrix} \tag{3.12}$$

After arithmetic manipulation we find

$$E_{out1}(t) = 0.5[E_{in}(t-\tau) - E_{in}(t)] \tag{3.13a}$$

$$E_{out2}(t) = j0.5[E_{in}(t-\tau) + E_{in}(t)] \tag{3.13b}$$

By considering that the delay time is τ =1 bit period. The power and shape of consecutive pulses in a phase modulated signal are similar. If we suppose that θ_1 and θ_2 are the absolute phases of two consecutive pulses, Equation (3.13) can be written as

$$E_{out1}(t) = 0.5E_{pulse}[e^{j\theta_1} - e^{j\theta_2}] = jE_{pulse}\sin\frac{\theta_1-\theta_2}{2}\exp\left(j\frac{\theta_1+\theta_2}{2}\right) \tag{3.14a}$$

$$E_{out2}(t) = j0.5E_{pulse}[e^{j\theta_1} + e^{j\theta_2}] = E_{pulse}\cos\frac{\theta_1-\theta_2}{2}\exp\left(j\frac{\theta_1+\theta_2}{2}\right) \tag{3.14b}$$

3.3.6 Balanced Detection

We can consider an ideal photodiode as a squared law component with low pass filtering, and the generated photocurrent I_{diode} when receiving optical signal with electric filed E_{in} is given by

$$I_{diode} = R\left|E_{in}\right|^2 \tag{3.15}$$

Where R is the responsivity of the photodiode.

In phase modulated systems two photodiodes can be used in a balanced detection setup in order to improve the receiver sensitivity and eliminate the noise of the receiver.

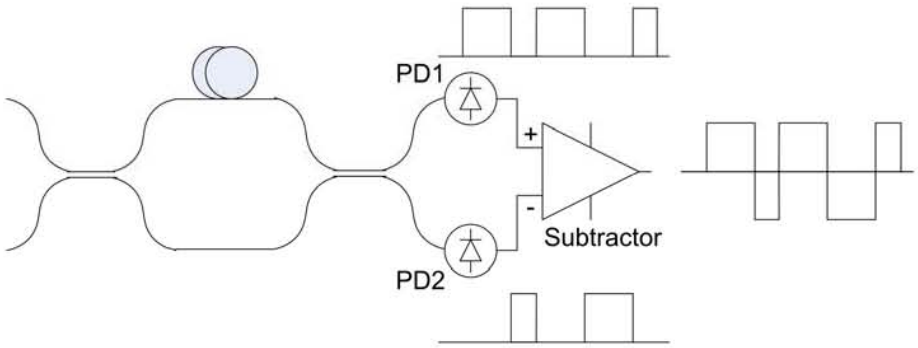

Figure 3.11. Balanced detection.

Figure 3.11 shows balanced photodiode detection. Two photodiodes are connected to the output arms of a MZI. Substituting Equation (3.14) to Equation 3.15, we get

$$I_{diode1} = R\left|E_{out1}(t)\right|^2 = RP_{pulse}\left|\sin\frac{\theta_1 - \theta_2}{2}\right|^2 \tag{3.16a}$$

$$I_{diode2} = R\left|E_{out2}(t)\right|^2 = RP_{pulse}\left|\cos\frac{\theta_1 - \theta_2}{2}\right|^2 \tag{3.16b}$$

Where P_{pulse} is power of the optical pulse.

After the subtracter, we get

$$I_{Subtractor} = RP_{pulse}\left(\left|\sin\frac{\theta_1-\theta_2}{2}\right|^2 - \left|\cos\frac{\theta_1-\theta_2}{2}\right|^2\right) \qquad (3.17c)$$

Based on Equations 3.16 we find that phase difference $\theta_1-\theta_2$ of consecutive bits can be found through the currents I_{diode1}, I_{diode2} and $I_{substractor}$.

Balanced photodiode detection gives 3dB SNR improvement when compared with single branch detection [33].

3.3.7 The Electronic Precoder for DPSK

The direct detection detector operates by mixing the phase modulated signal with a delayed version of itself. If we consider the sine arm as the detection output defined in equation 3.16b, then we find that when two successive bits have no phase difference logic "0" is induced, while it would be "1" if there is phase difference of π.

Table 3.1 Truth table of DPSK without a precoder.

$D_{in}(t)$	$D_{in}(t-T_b)$	$\theta(t)$	$\theta(t-T_b)$	$\theta(t)-\theta(t-T_b)$	$\left\|\sin\left(\frac{\theta(t)-\theta(t-T_b)}{2}\right)\right\|^2$
0	0	0	0	0	0
1	0	π	0	π	1
0	1	0	π	$-\pi$	1
1	1	π	π	0	0

In order to analyze the transmission logic of DPSK, Table 3.1 represents the system before adding a precoder, where $D_{in}(t)$ is original Pseudo Random Binary Sequence (PRBS) data to be transmitted through the system, $D_{in}(t-T_b)$ is one bit delay version of $D_{in}(t)$, θ is the phase shift keying corresponding to $D_{in}(t)$, $\theta(t)-\theta(t-T_b)$ is the phase difference of successive bits at the receiver, $\left|\sin\left(\frac{\theta(t)-\theta(t-T_b)}{2}\right)\right|^2$ is the output of the sine arm of the MZI defined in Equation (3.16a). According to Table 3.1, we find that

$$D_{out} = D_{in}(t)\overline{D_{in}(t-T_b)} + \overline{D_{in}(t)}D_{in}(t-T_b) \qquad (3.18)$$

This is a logic equation where D_{out} is the data of DPSK output, and a bar over a symbol means (NOT) logic.

Implementing the correct precoding to the transmitted data helps to achieve direct decoding at the receiver side without the need of a decoder, and for this purpose we need an electronic precoder at the transmitter side. Figure 3.12 shows the logical scheme of the required precoder for DPSK that corresponds to equation 3.16, and this precoder is used in all standard DPSK transmitters.

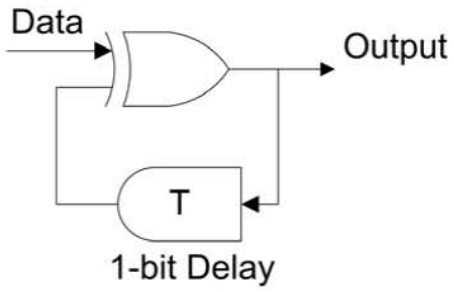

Figure 3.12. Electronic precoder for DPSK

3.4 Impairment to Phase-Modulated Optical Signal

In this section I give an overview of the main impairments to optical transmitted signal, which are mainly CD and BR, in addition to defining SPM as one of the nonlinear effects of optical fiber.

3.4.1 Fiber Chromatic Dispersion

The refractive index in dielectric materials depends on the frequency of the propagating light which results in chromatic dispersion. This is the same phenomenon which enables a glass prism to convert the wide spectrum sunlight into a rainbow.

For any optical modulated signal, there is a spectral bandwidth that the signal occupies. Due to CD, different frequencies of the bandwidth travel at different speeds. This results in limiting the transmission distance unless we use dispersion compensation.

The propagation of different spectral components inside an optical fiber follows the simple relationship of

$$B(z,\omega) = B(0,\omega)\exp[j\beta(\omega)z] \qquad (3.19)$$

- Z refers to the location on the fiber.
- $B(z,\omega)$ and $B(0,\omega)$ are the low pass representations of the signal spectra at the locations z or 0.
- $\beta(\omega)$ is the propagation constant as a function of the frequency of the optical carrier.

We define the group delay of the optical signal as

$$\upsilon_g = \beta_1^{-1} = \left(\frac{d\beta}{d\omega}\right)^{-1}\Bigg|_{\omega=\omega_c} \qquad (3.20)$$

The difference of arrival time is the dispersion coefficient [ps/km/nm]

$$D = \frac{d}{d\lambda}\left(\frac{1}{\upsilon_g}\right) = -\frac{2\pi c}{\lambda^2}\beta_2 \qquad (3.21)$$

The normal value for dispersion in a standard SMF at the wavelength window of 1.55 μm is around 17 ps/km/nm. In some systems Dispersion Shifted Fibers (DSFs) are used to shift the zero dispersion point to the 1.55 μm band, which helps in minimizing the dispersion along the fiber.

With a dispersion coefficient of D, two signals with wavelength difference of $\Delta\lambda$ travel by a time difference of $D\Delta\lambda L$ after a distance L. An approximation can be written

$$B(L,\omega) = B(0,\omega)\exp[j\frac{1}{2}\beta_2\omega^2 L] \qquad (3.22)$$

The system performance basically depends on the parameter $\beta_2 L B_d^2$ which is called CD index $\zeta = DLB_d^2$, where B_d is the data rate of the signal.

Figure 6 in [36] shows power penalty as a function of CD index with different modulation formats, NRZ-OOK, RZ-OOK, DPSK and 4-DPSK.

We notice in Figure 6 in [36] that DPSK has lower penalty than OOK when using either RZ or NRZ format. When comparing NRZ-DPSK and RZ-DPSK we find that for small dispersion values both have almost the same penalty of CD, while this changes with larger values of CD, as the penalty is much bigger for RZ compared to NRZ-DPSK, which is similar to the difference between NRZ-OOK, and RZ-OOK, this can be explained by the fact that RZ has wider power spectrum than NRZ in the main lobe.

In my experiment I used a low data rate of 2.5Gb/s, assuming a dispersion value of 17 ps/nm/km for SMF, and transmission distance of 20Km, we find that the CD index in my case is very low ~0.2, as Figure 6 in [36] shows in that region the dispersion index is very small such that all modulation formats have almost the same performance toward dispersion.

3.4.2 Self-Phase Modulation

For a pulse of light traveling along the fiber, there could be a difference in the value of refractive index at different points of the pulse based on its shape, and this causes a difference in the phase of the light of that pulse at different points, and this in turn translates to difference in frequency, therefore the spectrum of the pulse is broadened, this phenomenon is called SPM.

SPM can be represented by a chirp that is related to the shape of the pulse and the instantaneous level of powers along the pulse. A square pulse would suffer an abrupt change in power level at the leading and tailing edge, therefore the amount of produced chirp would be greater at the beginning and end of the pulse, and Gaussian pulses would suffer less chirp as their power scheme is gradual and even.

The phase change induced by SPM can be expressed as [37]

$$\Delta\phi = \gamma \Delta P L_{eff} \tag{3.23}$$

Where γ is the nonlinear coefficient of the fiber, ΔP is the intensity change of the signal, L_{eff} is the effective length of the fiber.

Due to the constant intensity for downstream in my experiment, the intensity fluctuation is near zero. Moreover, the power launched in the fiber is small as the transmission distance is limited 20 Km. Hence SPM in my system can be neglected.

3.4.3 Backreflection Effects in WDM-PONs

WDM-PONs use the same wavelength for both downstream and upstream for an efficient use of the optical spectrum. In addition to that they use one fiber for both directions of transmission to reduce cost which is called bidirectional transmission. However, this bidirectional transmission creates a technical issue, as the interference intensity noise coming from BR causes degradation in the Signal-To-Noise Ratio (SNR).

The noise of BR in WDM-PONs has been studied and researchers have analyzed the impact of both the BR of the downstream signal (Reflection-I), and the BR of the upstream signal (Reflection-II) on the loopback access network [38].
Due to their physical properties, all optical fibers have BRs all along the fiber, in addition to that actual access networks will include several reflection points such as splices and connectors, and those could produce stronger reflections if the connectors are dirty. The measured reflections for dirty connectors and splitters are shown in Table 3.2 [39]

Table 3.2: Optical Return Loss for UPC and APC connectors and splitters

	ORL
Open/Dirty UPC Connector	~ 15 dB
Dirty APC Connector	~ 22 - 31 dB
UPC Splitter	~ 33 dB
APC Splitter	~ 55 dB

Fig. 3.13 illustrates the BR signals in bidirectional access networks, we notice two types of BR that beat with the upstream signal, first is the reflected signal of downstream (BR I), second is the reflected signal of upstream which goes back into the ONU where it is remodulated and then travels again toward the OLT and it's called (BR II).

The upstream signal suffers from SNR degradation because of the interference with both BR signals, however the intensity noise caused by this interference can be reduced; it has been demonstrated that optimizing the signal amplification at the ONU can significantly reduce the SNR degradation due to BR [40], [41].

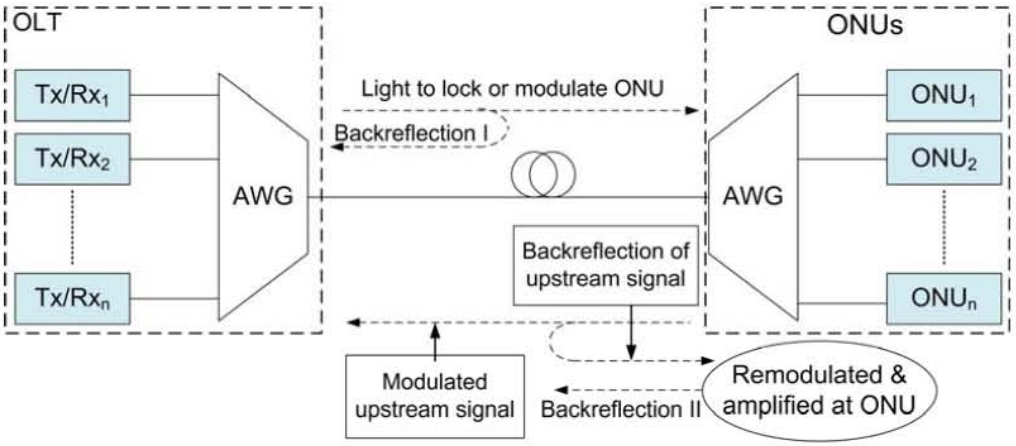

Fig. 3.13: Paths of two BR signals.

Fig. 3.14 shows how the SNR degradation due to BR I can be significantly reduced by amplification at the ONU. The horizontal and vertical axes represent transmission distance of the optical signal and relative optical power, respectively. As the figure shows, signal amplification at the ONU is necessary to achieve a large signal to Reflection-I power ratio because the optical power falls along the transmission path, and also the Reflection-I power level is constant.

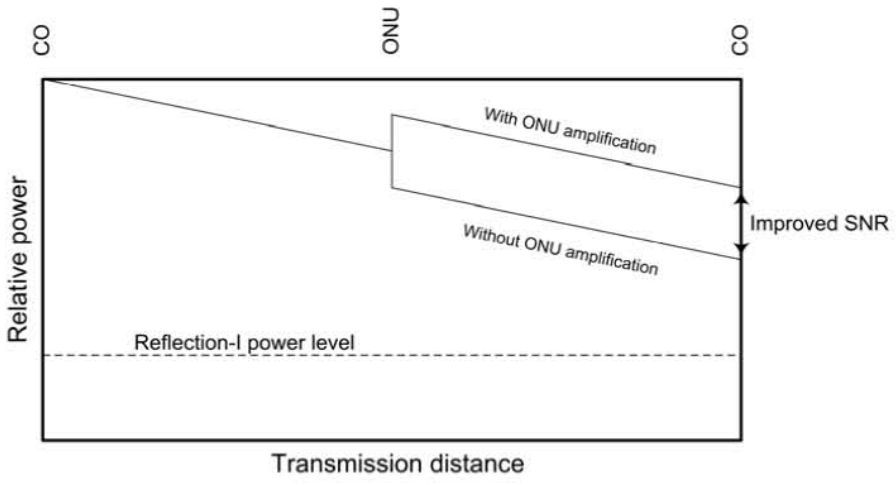

Fig. 3.14: Reducing the impact of Reflection-I by signal amplification at ONU

On the other hand, the effect of Reflection-II is also significant and must be taken into consideration specially at high values of ONU gain, and this limits how far we can go in increasing ONU gain in order to reduce the effect of BR I. Fig. 3.15 shows the relative received power at the receiver versus ONU gain (in decibel).

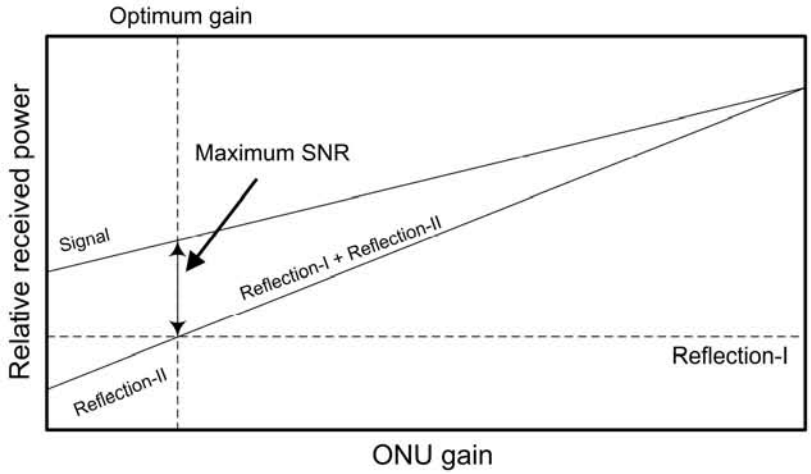

Fig. 3.15: Increase in the impact of Reflection-II with ONU gain

When we compare the signal power to Reflection-II power as a function of ONU gain, we find that while the signal power that is proportional to ONU gain, the power of Reflection-II is proportional to the square of ONU gain, and this is because the Reflection-II signal passes twice in the amplifier of the ONU.

As the figure shows, at low values of ONU gain Reflection-I would be the dominant BR noise, while Reflection-II is more dominant at high ONU gain, therefore choosing an optimal value of ONU gain helps minimize the overall penalty of BR in order to improve the received SNR.

It was found that the optimum ONU gain for a minimum BR penalty in the system in [38] is given by

$$G' = L' - 1.5 \qquad (3.24)$$

Where $G' = 10\log_{10}(g')$ and g' is the ONU gain that includes 3-dB modulation loss.

$L' = 10\log_{10}(l')$ where l' is the Transmission Line Loss (TLL).

More advanced model was developed in [42], and a formula was proposed to give the Relative Intensity Noise (RIN) of the beat noise for both downstream and upstream BR signals with the upstream signals:

$$RIN_{dn}(f) = \frac{8}{g\pi}\frac{\Delta\upsilon}{\Delta\upsilon^2 + f^2} ORL.e^{2\alpha L} \tag{3.25}$$

$$RIN_{un}(f) = \frac{4g}{\pi}\frac{\Delta\upsilon}{\Delta\upsilon^2 + f^2} ORL \tag{3.26}$$

g is the net power gain which includes the ONU gain as well as the component loss

$\Delta\upsilon$ is the linewidth of the laser source

f is the frequency

α is the fiber attenuation

L is the fiber length

ORL is the Optical Return Loss (ORL) of the fiber

Then the total beat noise optical power normalized to the signal optical power in the receiver bandwidth f_{bw} was given by

$$r^2(f_{bw}) = \int_0^{f_{bw}} RIN_{dn}(f)df + \int_0^{f_{bw}} RIN_{un}(f)df \tag{3.27}$$

The Q factor which is defined in [43] as the difference between the average value of the marks (ones) and of the spaces (zeros) divided by the sum of the standard deviations of the noise distributions around each. It is given by the following expression when beat noise is included:

$$Q = \frac{\Re P_{s-b}}{\sqrt{\sigma_{th}^2 + \Re^2 P_{s-b}^2 r^2(f_{bw})} + \sigma_{th}} \tag{3.28}$$

While the Q factor without including beat noise was given by

$$Q_o = \frac{\Re P_{s-0}}{2\sigma_{th}} \tag{3.29}$$

$\Re$ is the responsivity of the photodiode

P_{s-b} is signal power including beat noise

P_{s-0} is signal power without beat noise

σ_{th} is the thermal noise of the photodetector

The power penalty of BR was then given by

$$\delta = 10\log\frac{Q_o}{Q} \tag{3.30}$$

From (3.25) and (3.26) we can conclude that the BR penalty for both downstream and upstream increases in case of decreasing the linewidth of the laser source, or increasing the ORL of the fiber, while the effect of ONU gain (g) is different on each of BR penalty of downstream and upstream.

One should note that these models in [38] and [42] were developed for OOK only.
In my experimental work, I have carried out research to study BR in WDM-PONs in the remodulation scheme using both phase modulation and OOK in the network, as we will see later in Chapter 4.

Chapter 4

Experiments and results

4.1 A Novel Remodulation Scheme for WDM-PONs Employing Phase Modulation for Both Downstream and Upstream

4.1.1 Motivation

As mentioned in chapter 2, signal remodulation is one of the solutions that aim to decrease the cost of WDM-PON deployment by saving the need for a laser source at the ONU; hence the ONU uses the same downstream signal as a carrier for upstream data. Several remodulation architectures have been proposed, including the use of OOK for both downstream and upstream [44]; downstream low Extinction Ratio (ER) OOK and upstream DPSK [45]; downstream DPSK and upstream OOK [46], However, these approaches have several disadvantages, such as high chirp [44],[46], limited speed [44]-[46], and reduced ER [45].

Another system has been recently proposed using a Reduced Modulation Depth (RMD) DPSK for downstream signal and a Full Modulation Depth (FMD) DPSK for upstream signal [47], and this approach has a limitation on the downstream transmission of both the RMD and that balanced detection can not be used in it because this approach is remodulating all the output signal of the constructive port of the Delay Line Interferometer (DLI) while it detects downstream data at the destructive port only, the former limitation makes it less tolerant toward phase errors in the DLI [48], while the latter makes it lose the DPSK +3dB advantage over OOK for downstream link that comes only with balanced detection [49].

In this work, I propose a novel wavelength remodulation scheme for WDM-PON using DPSK with FMD for both downstream and upstream signal. I demonstrate the system at 2.5 Gb/s in both directions due to available equipments I currently have, however the system is robust toward dispersion as I show in the experimental results, therefore the same principle could be applied to higher speed systems.

Driving the phase modulator with RZ data to produce the downstream signal enabled me to remove all downstream phase information in the ONU using a pulse carver, such that I could write the upstream phase information on the signal coming from the OLT with no phase information, the system has also the advantage of using either single ended or balanced detection unlike prior remodulation schemes [47], [48].

4.1.2. Operation principle:

The operation principle of the proposed system is illustrated in Fig. 4.1. In the OLT, I modulated the light of a laser source using a phase modulator driven by an RZ pre-coded data with a duty cycle of 50%, and this causes writing phase information on the first half of each bit leaving the second half without phase information.

At the ONU side, a portion of the downstream signal is detected using a DPSK receiver which restores downstream data in RZ format. The rest of the signal is passed through a pulse carver which is a device usually implemented as sinusoidally driven MZMs such that it removes the phase-modulated slots of the downstream signal leaving only the un-modulated slots. Subsequently, the phase free-signal is passed through another phase modulator at the ONU. This modulator is driven by the upstream data signal. This signal is NRZ and is differentially pre-coded using a DPSK pre-coder.

The upstream signal exits the ONU as a standard RZ-DPSK that can be transmitted up the link to the OLT to be detected using any DPSK receiver.

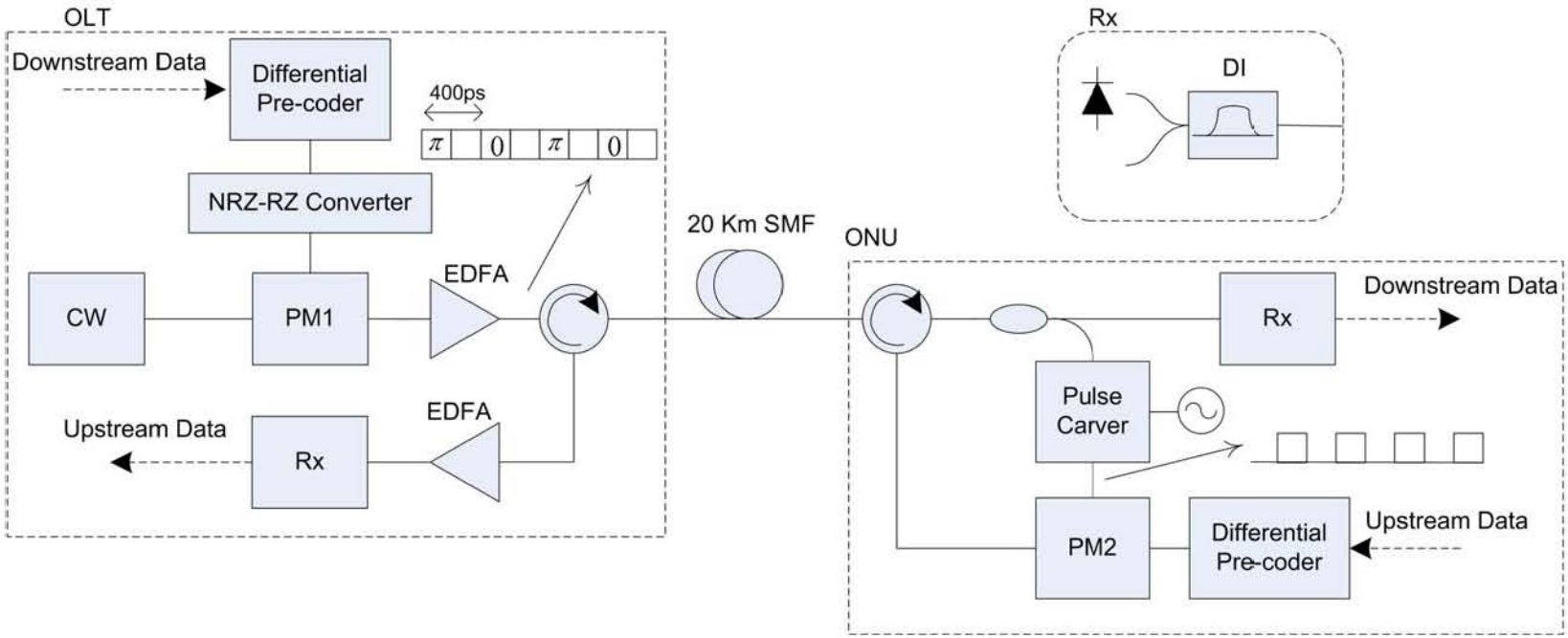

Fig. 4.1. Principle and experimental setup of the proposed remodulation system. PM: phase modulator, SMF: single mode fiber, EDFA: erbium-doped fiber amplifier, DI: delayed interferometer, Inset: DPSK receiver

4.1.3. Experimental setup and results

A schematic diagram of the experimental setup for the proposed remodulation system is shown in Fig. 4.1. At the OLT, the downstream 2.5Gb/s DPSK signal was generated by using a continuous-wave light source at 1549.1 nm that passes into a $LiNbO_3$phase modulator driven by an RZ signal. This signal was generated by converting a 2.5Gb/s NRZ PRBS data stream with a length of $2^{23}-1$ to a 50% RZ signal. The use of 50% RZ produces un-modulated slots that are 200ps wide. I did not actually use a pre-coder in the experiment because the data is random and it would not make any difference. The generated DPSK signal is passed through an optical bandpass filter with a 3dB bandwidth of ~0.8nm which emulates one channel of a 100 GHz AWG, and amplified to 7dBm using an EDFA then launched into a 20 km standard SMF using an optical circulator.

At the ONU side, and after passing the received signal through a circulator I split it using a 20:80 optical coupler, taking 20% of the light to a downstream receiver shown in the inset in Fig. 4.1 to obtain downstream data in an RZ format, because interfering every two un-modulated slots together will produce no power at the output. The rest of light is fed into a 2.5 GB/s Bias-Ready JDSU intensity modulator driven by a 2.5 GB/s clock source, which plays the role of a pulse carver. I used an RF phase-shifter with the clock stream to adjust the process of removing data slots which are contained in the downstream signal. The signal then becomes an RZ of a 50% duty cycle with no phase information and a power level of -8.9dBm. I passed this signal into another $LiNbO_3$phase modulator driven by a 2.5GB/s NRZ data stream which is also PRBS data with a length of $2^{23}-1$ to obtain the RZ-DPSK upstream signal with -13.5dBm which is in turn launched into the 20 km SMF using the circulator at the ONU side. I received this signal at the OLT side by amplifying it with an EDFA and then passing it through a DPSK receiver which has the same structure as the one I used to receive the downstream signal.

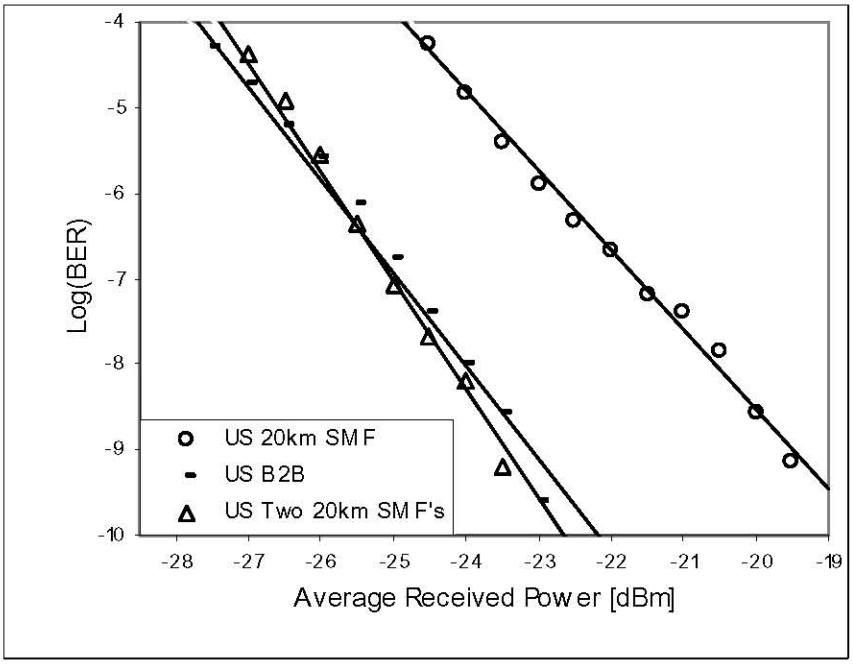

(a)

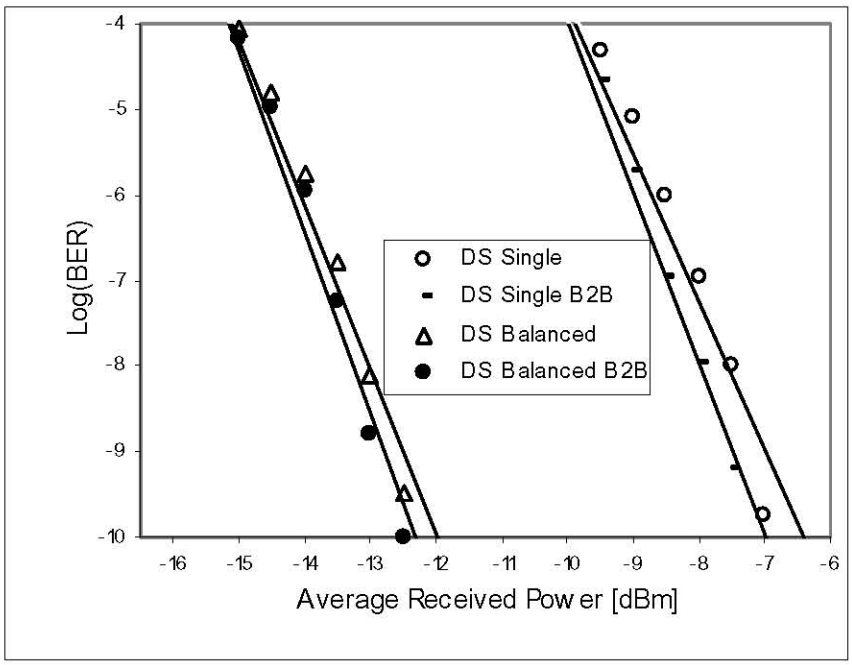

(b)

Fig. 4.2. 2.5-Gb/s BER measurements of (a) upstream signals in the cases of using single-fiber configuration, dual-fiber configuration and B2B, (b) downstream signals in both single ended and balanced detection in the two cases of using single-fiber configuration, and B2B.

The Bit-Error-Rate (BER) measurement results for both downstream and upstream signals are shown in Fig. 4.2. For single ended detection I used a PP-10G Nortel receiver while for balanced detection I used a Limiting TIA Discovery

Semiconductors Balanced Detector. to investigate the issue of Rayleigh noise on the upstream signal, I measured the BER in both the cases of single-fiber and dual-fiber configuration.

In the upstream I measured a receiver sensitivity at BER=10^{-9} in the case of single-fiber -20.4 dBm compared to -24.2 dBm in the dual-fiber case and -23.9 dBm in the Back-To-Back (B2B) one, which means that the dispersion penalty alone is minimaland ~3.5dB penalty coming from BR and dispersion together [48]. As for the downstream I measured a receiver sensitivity at BER=10^{-9} in the case of single ended detection around -7.4dBm for both B2B and single-fiber, while there was around ~5dB advantage in receiver sensitivity for balanced detection over single ended detection. The limitation in the receiver sensitivity for downstream compared to upstream comes from the photodetector itself rather than the system.

While the pulse carver in my setup adds cost and complexity to the ONU compared to the scheme discussed in [47], it should be noted that the pulse carver can be integrated with the phase modulator and does not need to be wide band. In addition, the setup in [47] has more tolerance to BR by using RMD downstream signal and hence it has narrower optical spectrum that can be filtered out by using the destructive port at the OLT receiver, however their setup suffers higher penalty because of the beating between downstream data and upstream data at the receiver side, while in my setup downstream data is removed by the pulse carver at the ONU before remodulating the signal. Moreover my setup has ~6dB advantage in receiver sensitivity for upstream. My scheme also offers the option of using a balanced receiver for downstream, for a higher cost.
The use of electrical RZ for downstream was also studied in [50], and while it has higher tolerance to BR than my setup for the same reason of RMD in [47], it has an overall ~3dB less receiver sensitivity for upstream.

Fig. 4.3 shows the eye diagrams for upstream and downstream in both single ended and balanced detection. We notice ripples at the zero level inside the eye in (d) I show them more clearly in (e) which we obtain by stopping the data of upstream while keeping all the system working. These ripples are caused by the imperfect removal of downstream data by the intensity modulator, as the latter is driven by a sinusoid signal, rather than an ideal squared signal.

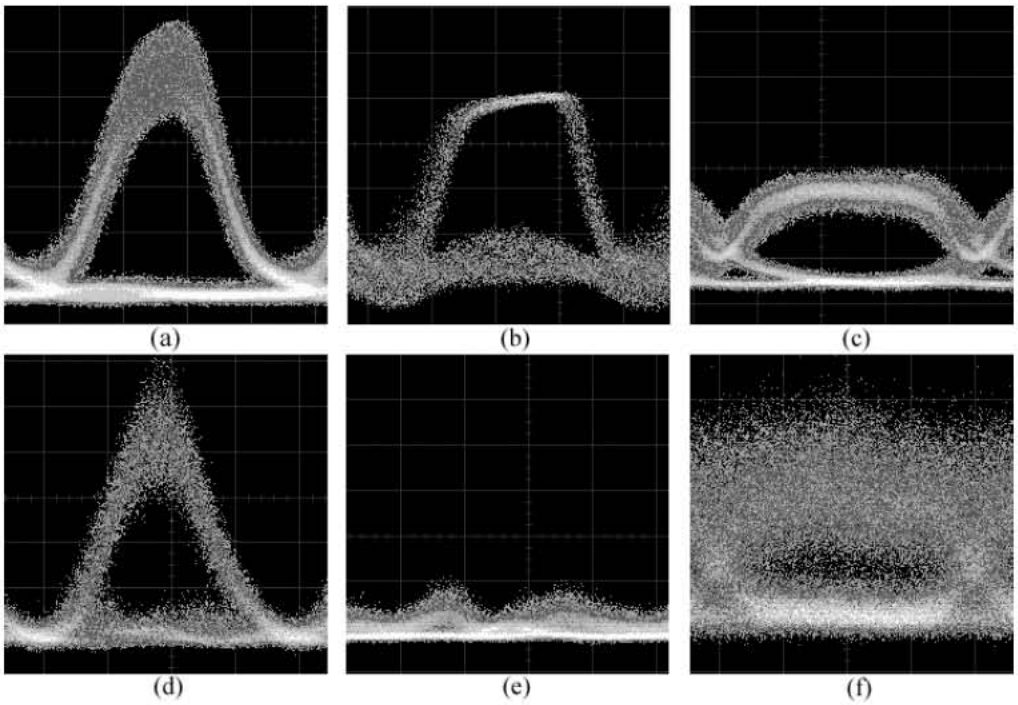

Fig. 4.3 Eye diagrams of the downstream and upstream signals. (a) Downstream - single ended (b) Downstream - balanced (c) Downstream single ended with DPSK-OOK (d) Upstream single ended (e) Upstream signal when stopping upstream data with single ended detection (f) Upstream with DPSK-OOK

To compare my system with the conventional scheme that uses DPSK for downstream and OOK for upstream, I show in Fig. 4.3 the eye of downstream DPSK (c) and the eye of upstream OOK in (f), we notice a significant advantage in the upstream case, and this is gained by the technique used in my setup as all downstream data is removed by the pulse carver at the ONU while in the case of DPSK-OOK downstream data will travel with upstream data and suffer different impairments along the transmission path causing severe degradation in the quality of the received signal.

4.2 Impact of backreflections on bidirectional WDM-PONs with wavelength remodulation schemes

4.2.1 Motivation

Recently, several remodulation architectures which include the advanced modulation format such as DPSK have been proposed. In these schemes, OOK is used for the downstream signal and DPSK is used for the upstream signal or vice versa [46]. Since the data information of downstream and upstream is separately carried on amplitude or phase, it is not necessary to sacrifice ER. However, these approaches still have the disadvantages such as high chirp and limited data rate [44, 46]. To overcome these disadvantages, a remodulation scheme using DPSK for both downstream and upstream has been proposed using RMD for downstream signal [47]. I have also proposed a WDM-PON system lately using DPSK for both downstream and upstream, in which FMD DPSK for both signals are realized [51].

In all of these proposed WDM-PON configurations, bidirectional transmission with only one single fiber is used to reduce cost and accelerate PON deployment. However, such bidirectional loopback transmission results in beat noises between BRs and the signal since they have the same wavelength, i.e., the backreflected up/downstream beats with its counter-propagating down/upstream, which leads to degradation of the system performance as I showed in Fig. 3.13. In [3], I have analyzed the system impairment due to beat noises between BRs and the upstream signal in bidirectional single-fiber WDM-PONs, where the seed light of the upstream is either CW or intensity modulated downstream and the upstream uses OOK modulation. It was demonstrated that there is an optimum ONU gain to minimize the impairment of BRs, which is determined by the TLL, the linewidth of the seed light, the chirp effect at the ONU as well as the receiver bandwidth.

In this work, I focus on the investigation of BR impairment in WDM-PONs with remodulation scheme when using DPSK modulation format for both downstream and upstream. To the best of my knowledge, this is the first experiment to explore BR penalty in remodulated WDM-PONs that employ advanced modulation formats. I demonstrate that in WDM-PONs with DPSK remodulation scheme, the power penalty caused by the beat noises is also dependant on the ONU gain, the TLL, the

linewidth of the seed light, and the modulation depth of the downstream signal, in addition, I show the interesting role of the destructive port of DLI with the backreflected signal of downstream which does not apply to the constructive port.

4.2.2 Experiment and results

As described in section 3.4.3, there are two dominant sources of BRs which beat with the upstream signal in a single-fiber bidirectional WDM-PON system with remodulation scheme. As depicted in Fig.3.5, one is the BR of the downstream signal (BR I), and the other is the remodulated and reamplified BR of the upstream signal (BR II). The experimental setup to investigate the impacts of these BRs is shown in Fig. 4.4 and it uses the same method as [3] for analyzing BR [3]. The only difference is that in [3] the modulation scheme is OOK for both the up and down streams while I used DPSK for both.

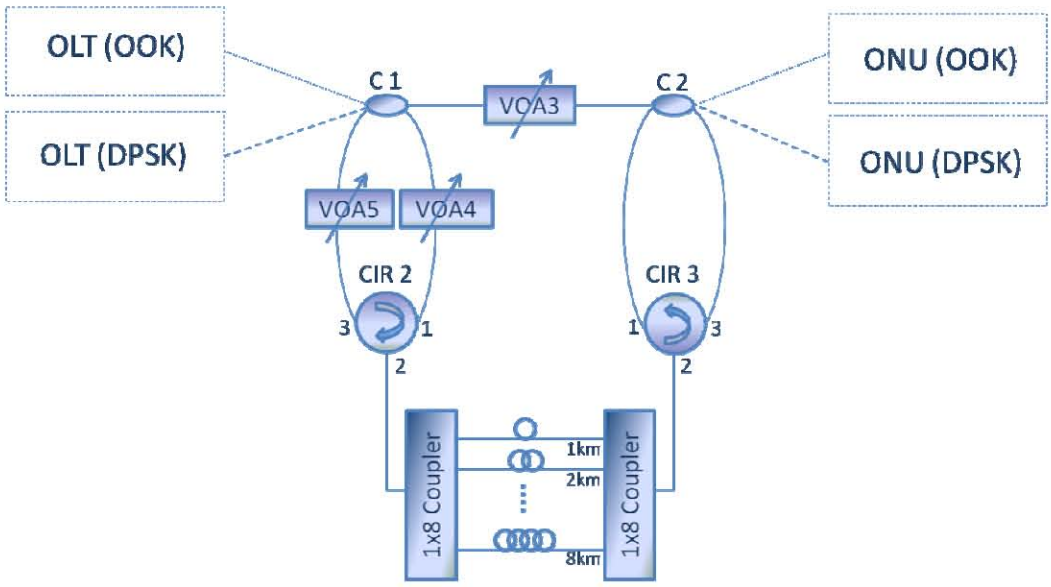

Fig 4.4. Schematic diagram showing the standard method that is used to analyze BR with either OOK or DPSK modulation format

Fig. 4.5 shows a detailed schematic of the setup that I used in the experiment. The OLT is composed of a laser source, a phase modulator driven by RZ data, an optical receiver Rx, an EDFA, and a Bit Error Rate Test set (BERT). Variable Optical Attenuator (VOA1) is used to change the injection signal power to the ONU while VOA5 is for measuring the power penalty after introducing the BRs. The ONU includes a pulse carver (intensity modulator), a phase modulator for writing upstream

data, two EDFAs, a VOA and a circulator. The ONU gain is altered by tuning VOA4 at the ONU. The rest of the system is the transmission line, which consists of 3dB couplers, VOAs, polarization controllers, circulators, 1x8 couplers and Optical Delay Lines (ODLs).

In this experimental setup, I simulated both BR I and BR II at the same time by only one set of delay fibers (1km-8km), as shown in Fig. 4.5. Since these delay fibers vary in lengths (i.e., they have different delay times), they could represent the discrete reflection points in the transmission line, which approximately simulates the continuous distributed reflection. The path of BR I is as follows: The output light from the OLT goes to port 1 of circulator 2 through the 3dB coupler 1, and then it is delayed by the ODLs, goes back to OLT after circulator 3, coupler 2 and coupler 1.

BR II goes the opposite direction to BR I through the ODLs. It starts from 3dB coupler 2, and then arrives at port 1 of circulator 3. After being delayed, it goes back to ONU, and then it is remodulated, reamplified and sent back to OLT. The transmission line is composed of the coupler 1, coupler 2 and attenuator 1. Therefore, the TLL could be changed by attenuator 1. Attenuators 2 and 3 are in charge of adjusting BR I and II, respectively. As in a real single-fiber bidirectional PON system, the ORL of the OLT and the ONU are the same, it is important to verify that this condition is satisfied.

In my setup, the ORLs are measured at the outputs of the OLT and the ONU respectively. The ORL of the OLT is measured to be the optical power difference of the signal output of the OLT and the coming back signal after the ODLs. The ORL of the ONU is measured the same way at the output of the ONU. Please note that when measuring the ORL at the OLT side, the ONU is not operational. The same condition applied to the measurement of the ORL at the ONU side. Unlike the previous work of [3], and instead of measuring the power penalty at the OLT receiver to characterize the impact of the beat noises, I used the difference of Log(BER) of the received upstream signal for different values of ONU gain before and after applying BR signals. The BERT was used to monitor the BER change during the measurement. It should be noted that all results were measured at TLL of 7 dB and receiver bandwidth of 10 GHz unless stated otherwise.

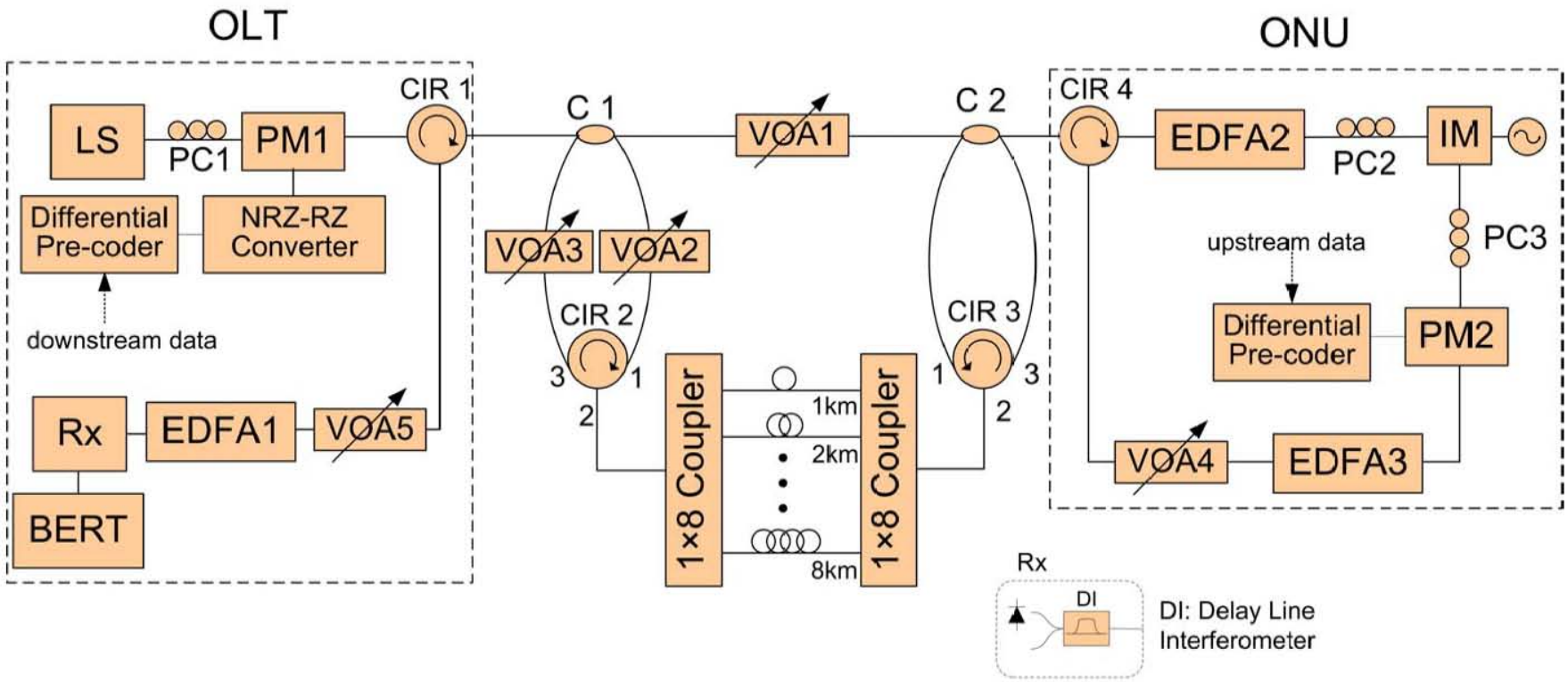

Fig. 4.5. Schematic diagram of the setup used to analyze BR penalty in WDM PON when using phase modulation for both downstream and upstream. PM: Phase modulator, IM: Intensity modulator, LS: Laser source.

Fig. 4.6 depicts the BR penalty as a function of ONU gain at different values of ORL 27.5, 29, and 31 dB, and it demonstrates that higher ORL results in higher penalty as expected from the theory in equations (3.25) and (3.26). It also shows that there is an optimum value for ONU gain that minimizes the BR penalty. As seen in the figure, this value is between 4 and 5 dB which is close to (5.5dB) that is expected when applying equation (3.24) with TLL of 7dB in my case

Fig. 4.7 shows the eye diagram of upstream signal also at different values of ONU gain taken at -1, 5, and 17 dB, we notice that the quality of the eye is best at 5 that is the optimum ONU gain for the least BR penalty.

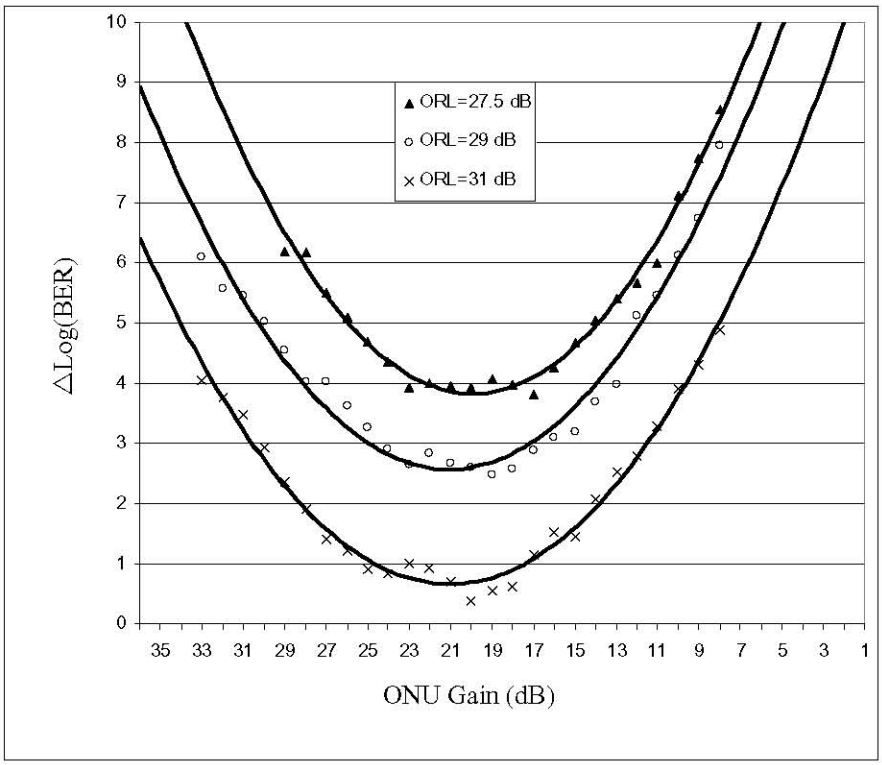

Fig. 4.6 BR penalty with different optical return loss values

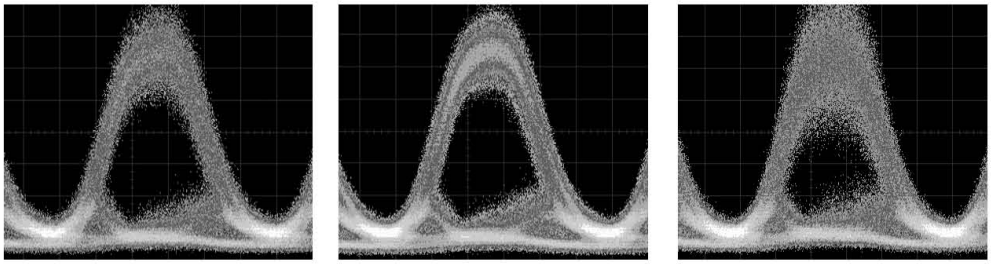

Fig. 4.7 Eye diagram of received upstream signal at different values of ONU gain:
(a) gain=-1dB (b) gain=5dB (c) gain=17dB

To verify the effect of TLL on BR penalty in the system, the variation of penalty as a function of ONU gain is shown in Fig. 4.8 for TLL of 7 and 9dB with both measurements taken at 30.2 dB ORL, we can see that higher TLL causes higher penalty of BR in the system which is consistent with what is expected from theory in case of OOK [42].

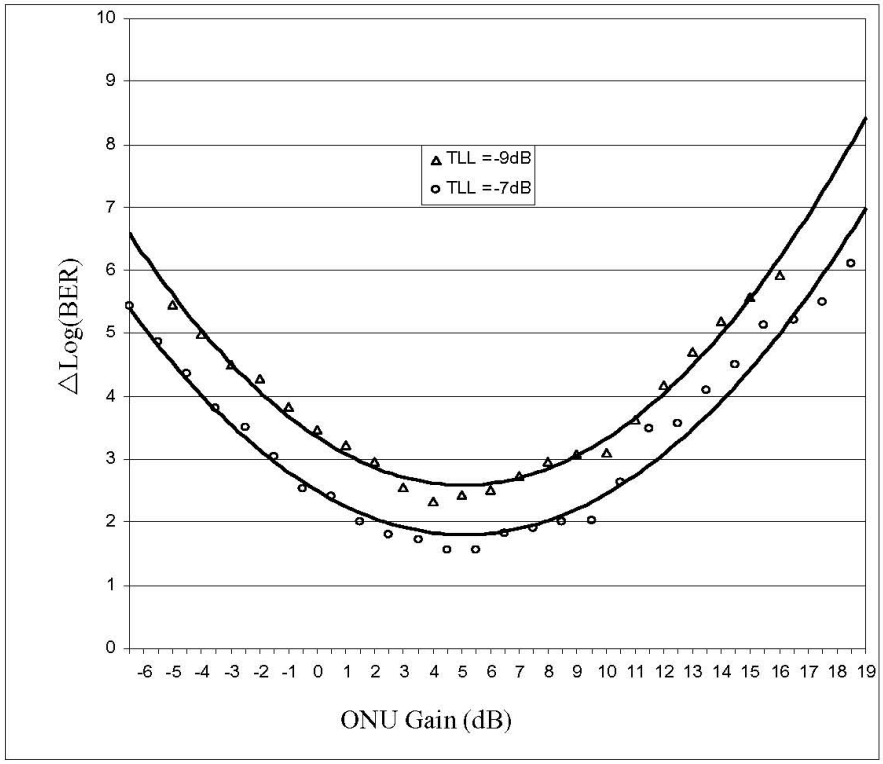

Fig. 4.8 BR penalty with different transmission line loss values

The bandwidth of the receiver was also investigated in its effect on the penalty, based on the theory [42], it is expected that as the bandwidth decreases the beat noise will decrease and the BR penalty decrease. In my experiment I tested two values of

receiver bandwidth namely 3GHz and 10GHz with both taken at 29.9 dB ORL. As depicted in Fig. 4.9 I could not see any difference between the two receiver bandwidths. I believe that this is because the BW that I tried was higher than the data rate of 2.5 GB/s. I attempted to use a lower bandwidth than 3 GHZ by using an electrical filter with lower cut off frequency (1.25 GHz), the signal quality was severely affected, and therefore I did not continue that test.

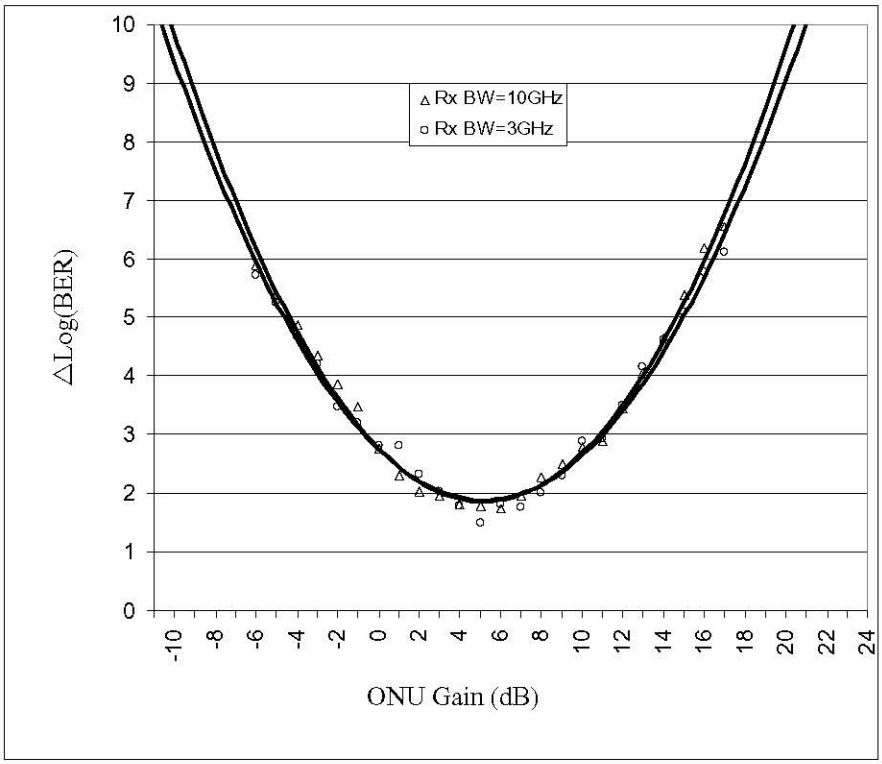

Fig. 4.9 BR penalty with different receiver bandwidths

Fig. 4.10 shows BR penalty as a function of ONU gain for different conditions of downstream modulation, FMD, RMD, and CW all taken at 30 dB ORL. The results seemed contrary to my expectations, as the CW penalty seems to be significantly lower than FMD, even though CW has a smaller effective linewidth and expected to be having higher penalty [42]. In addition we notice in CW case the optimum ONU gain is lower than that in FMD by around ~8dB. To further investigate this issue I measured the BR penalty by measuring BR I and BR II separately for different cases of downstreams. This includes CW, FMD, and FMD with removing the electrical filter (5.4GHz) that was applied to the downstream data Fig. 4.11. This filter limits

the bandwidth of downstream data when applied, and it represents a case that comes in between the CW and the FMD in terms of bandwidth.

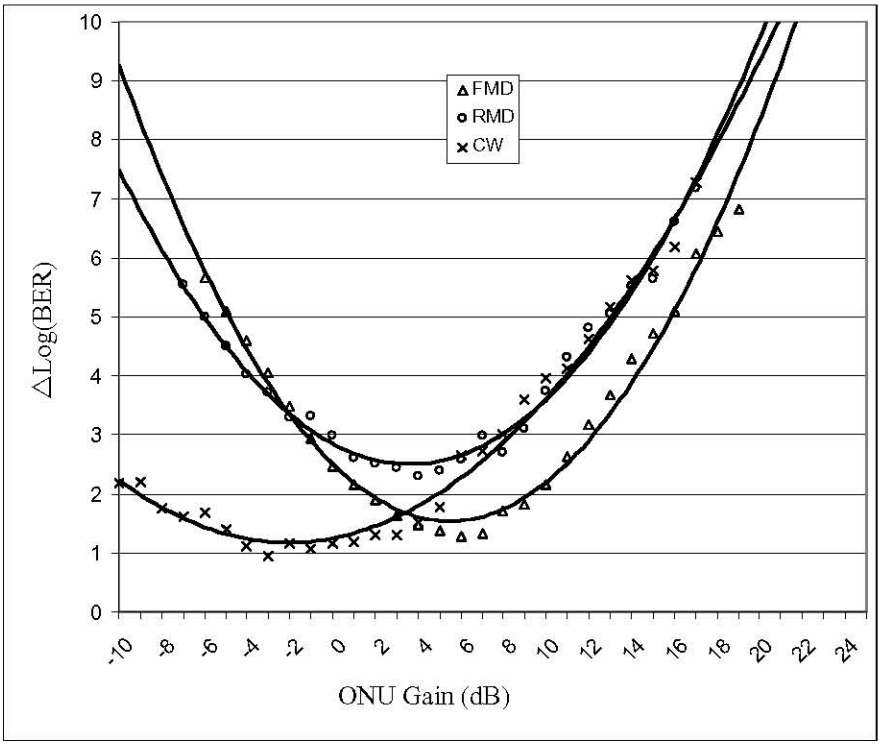

Fig. 4.10 BR penalty in case of: Full modulation depth, reduced modulation depth of the downstream signal and also in case of continuous wave downstream (CW downstream)

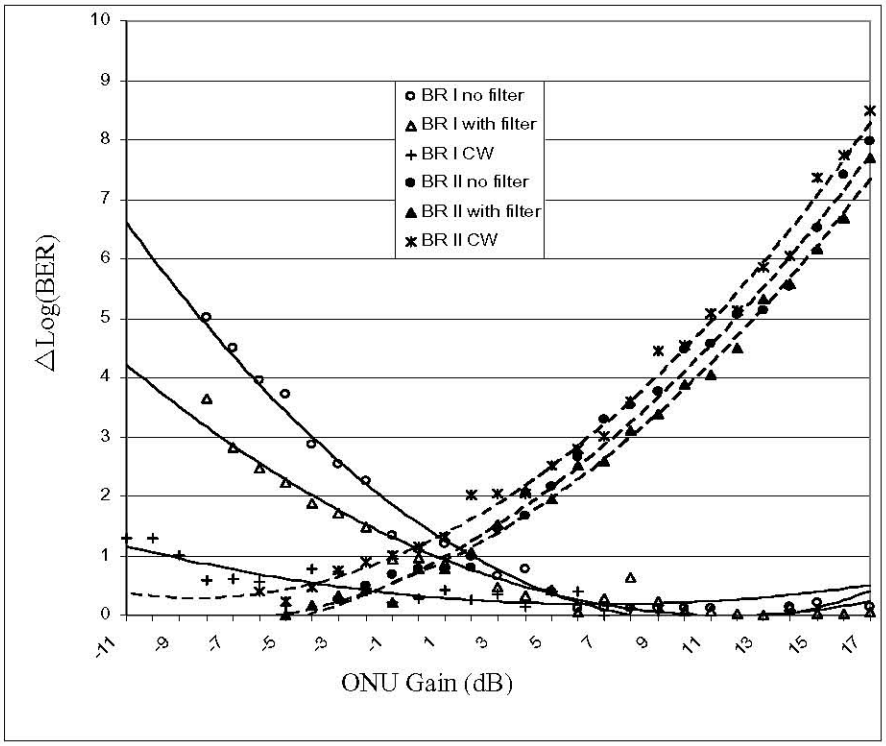

Fig. 4.11 BR penalty type I and II in case of: Full modulation depth with filter on downstream data, full modulation depth without filter on downstream data and also in case of continuous wave downstream (CW downstream) when using SMFs, ORL=31.1 dB

In Fig. 4.11 we notice that for BR II (the right hand part of the figure), CW is the highest which meets the BR theory of OOK in [42], and for the two cases of FMD with and without filter there is no significant difference between them, which means that BR II is not much affected by the modulation of downstream signal, because BR II results from the reflected signal of upstream that returns to the ONU where it is modulated for the second time and then sent again to the OLT to beat with the upstream signal at the receiver side as I explained before. The situation is different for BR I, as we can notice that the penalty in case of (with filter) is lower than (without filter).

The dependence of the BR penalty on the bandwidth of the downstream signal directed my attention to the possibility of coupling between BR and dispersion. In order for me to test such a possibility I changed the fiber type in the setup and used 8 DSFs instead of the SMFs and I repeated the tests. I argue that if there is no coupling between dispersion and BR, the BR penalty should remain the same irrespective of the fiber type. This is because my penalty of BR is calculated by measuring the BER

including BR and subtracting it from the BER without applying BR. The results are shown in Fig. 4.11 for SMF fibers and Fig. 4.12 for DSF.

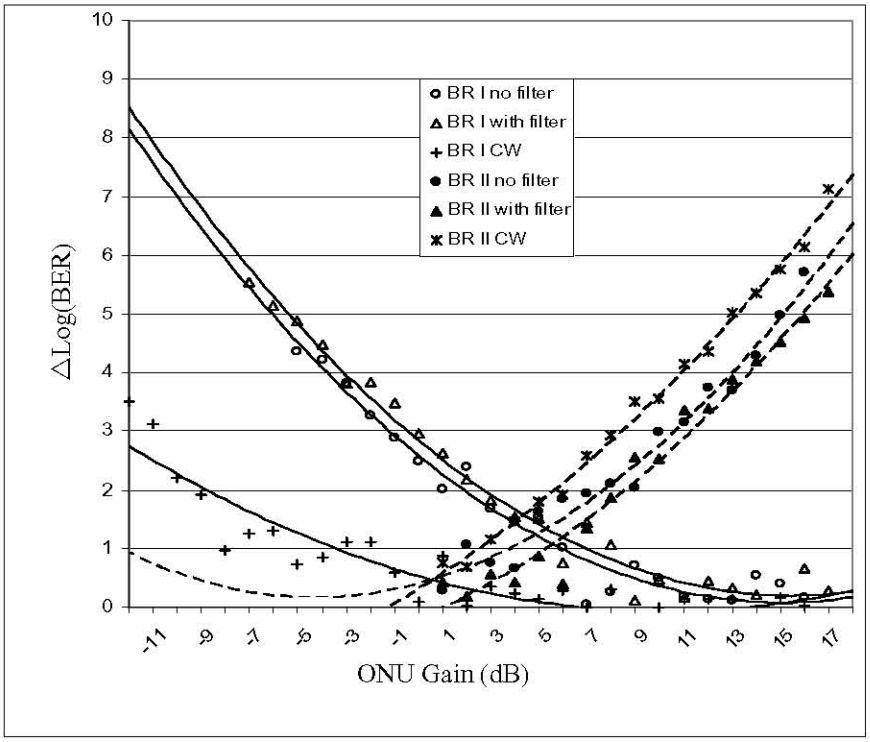

Fig. 4.12 BR penalty type I and II in case of: Full modulation depth with filter on downstream data, full modulation depth without filter on downstream data and also in case of continuous wave downstream (CW downstream) when using DSFs, ORL=30.1 dB

As Fig. 4.12 shows, the results of BR II did not change much when compared to the results when using SMFs shown in Fig. 4.11, while there is a clear difference in the penalty of BR I for the different signals. The penalty in case of using filter (smaller bandwidth) is now a little higher than the penalty without filter and this proves the point of coupled effect of dispersion with BR. Practically, this issue is very important, as researchers follow a standard technique to find the penalty of BR in systems which assumes that the BR penalty and dispersion penalties are independent [50]. Based on this assumption, they compare the power penalty of two cases of B2B transmission and the case of two separate fibers for downstream and upstream, and by this they find the dispersion penalty (no BR penalty in case of two fibers), and then they do a test with a bidirectional fiber, where BR penalty is added, and by this they find the value of BR penalty in the standard case of bidirectional fiber transmission.

However the results in Fig. 4.11 and 4.12 clearly demonstrates that this method is flawed, because the penalty in case of one fiber results from dispersion, BRs, in addition to the penalty of dispersion hitting BR signals, thus the difference in penalty between the two cases of one fiber and two fibers represents a penalty of BR coupled with the penalty of additional dispersion. Consequently separating downstream from upstream is not a correct method to find BR penalty, and researchers need to use other methods like using dispersion compensation in case of bidirectional fiber transmission then comparing with the case of normal transmission without dispersion compensation and find the difference between these two.

To confirm this claim I implemented a test that emphasizes the penalty induced from BR I when using a filter for different wavelengths while using DSFs, such that the comparison is done under same conditions but with different values of wavelengths and therefore different values of dispersion in the system, and I found the results shown in Fig. 4.13

We can see that the penalty of BR varies for different values of dispersion in the system (using different wavelengths is equivalent to applying different dispersion values to the signals), which means that the two penalties of BR and dispersion are coupled together and can't be separated except by using DSFs or dispersion compensation in the transmission system.

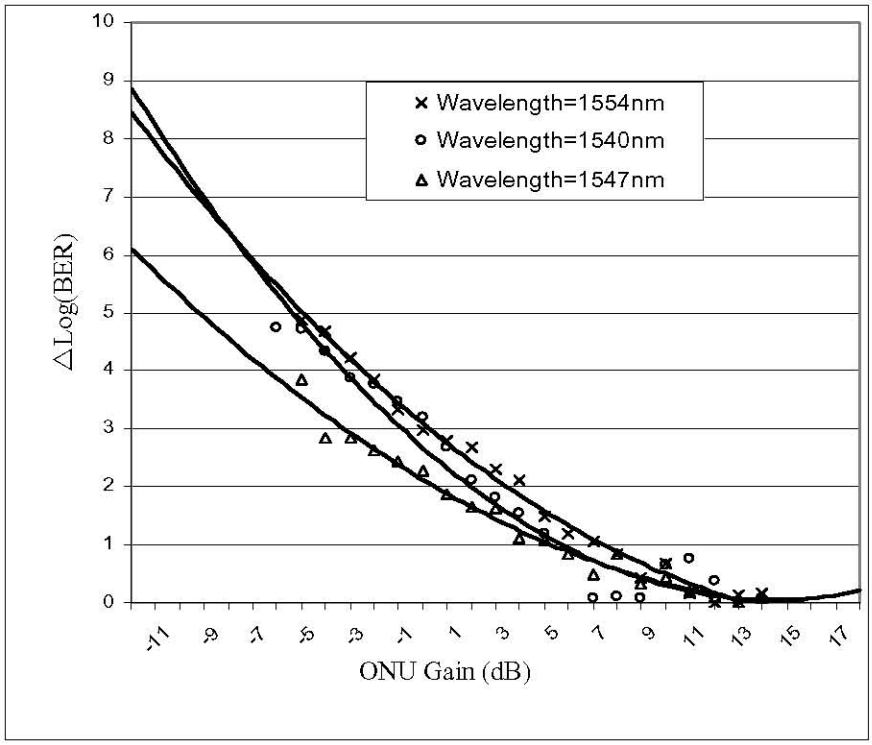

Fig. 4.13 BR penalty type I in case of FMD downstream signal when using a filter on downstream data with different values of dispersion, ORL=29.8 dB

In addition to the penalty of BR and dispersion that are coupled in my system there is a third factor that plays a significant role in determining the value of penalty induced, as the former two penalties can't explain why the penalty of CW is the lowest in Fig. 4.10, 4.11 and 4.12, while it is supposed to be the highest, because it has the smallest bandwidth, so the BR penalty should be at maximum value, and it does not suffer dispersion. I found that this is coming from the role of the destructive port of DLI which I was using in all my measurements.

The destructive port of the DLI acts like a notch filter toward the optical signal, and it suppresses a signal depending on its bandwidth, therefore smallest bandwidths suffer more suppression by the destructive port of the DLI. In Fig 4.10 the BR CW signal is significantly suppressed by the DLI and this effect pulls the curve down to the lowest value among the other cases, and for the RMD signal in comparison with the FMD it has a smaller bandwidth, and its penalty is the overall of three factors: dispersion which is smaller than that of FMD, BR which is higher than that of FMD, and the suppression of the DLI, and the result is the penalty that we can see in Fig 4.10.

I found that the role of the destructive port of DLI in suppressing BR of CW signals has already been investigated in the application of carrier-distributed WDM-PONs in which the carrier of upstream is sent as CW from the OLT in addition to the modulated downstream signal [52], [53].

To confirm the role of the destructive port of the DLI in suppressing BR CW signals I measured the penalty of BRI in case of using each of the ports of the DLI, and I show the results in Fig. 4.14. We can see a significant difference in the penalty between the two cases.

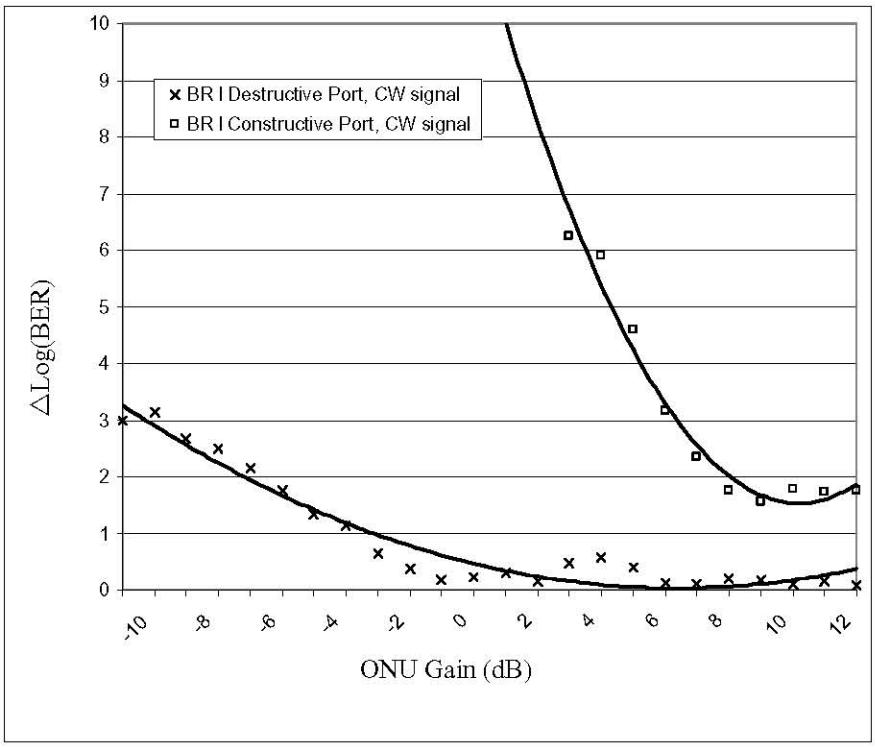

Fig. 4.14 BR penalty type I in case of using the destructive port of the DLI or the constructive port, ORL=29 dB

To further clear out the role of the three different factors in the BR penalty measurements that I obtained using the destructive port, we can write the following:
From (3.22) we can write the transfer function of a lossless fiber when considering only CD as impairment to the backreflected optical signal as

$$H_f(\omega) = \exp(-j\frac{L}{2}\beta_2\omega^2) \tag{4.1}$$

The transfer function of the destructive port of the DLI could be written as:

$$H_d(\omega) = 0.5[-1 + \exp(-j\omega T)] \tag{4.2}$$

Where T is the delay period of the DLI.

If we take $S_b(\omega)$ as the power spectral density (PSD) of the backreflected signal then the average of reflection power at the input of the DLI could be written as:

$$P_r = \int_{-\infty}^{+\infty} S_b(\omega) d\omega \tag{4.3}$$

And the average reflection power at the DLI's destructive port is then:

$$P_r' = \int_{-\infty}^{+\infty} H_f(\omega) H_d(\omega) S_b(\omega) d\omega \quad \Rightarrow$$

$$P_r' = \int_{-\infty}^{+\infty} 0.5[-\exp(-j\frac{L}{2}\beta_2\omega^2) + \exp(-j(\omega T + \frac{L}{2}\beta_2\omega^2))] S_b(\omega) d\omega \tag{4.4}$$

Equation (4.4) shows that the reflection power at the destructive port of the DLI is related to CD, the backreflected signal itself, and the transfer function of the destructive port of the DLI.

To study the effect of linewidth on the penalty induced by BR, I used two laser sources with different linewidth 0.1 MHz, and 1 MHz, and I found that the smaller the linewidth is, the higher the penalty of BR as shown in Fig. 4.15, which meets the theoretical analysis in [42] and the results in [3], in addition we can see that the optimum ONU gain in case of 1 MHz linewidth source is almost 4 dB smaller than the optimum ONU gain in case of 0.1 MHz linewidth laser source, as for the role of DLI suppression in this case, one should note that the difference in linewidth between the two cases is too small to make any difference in suppression [53].

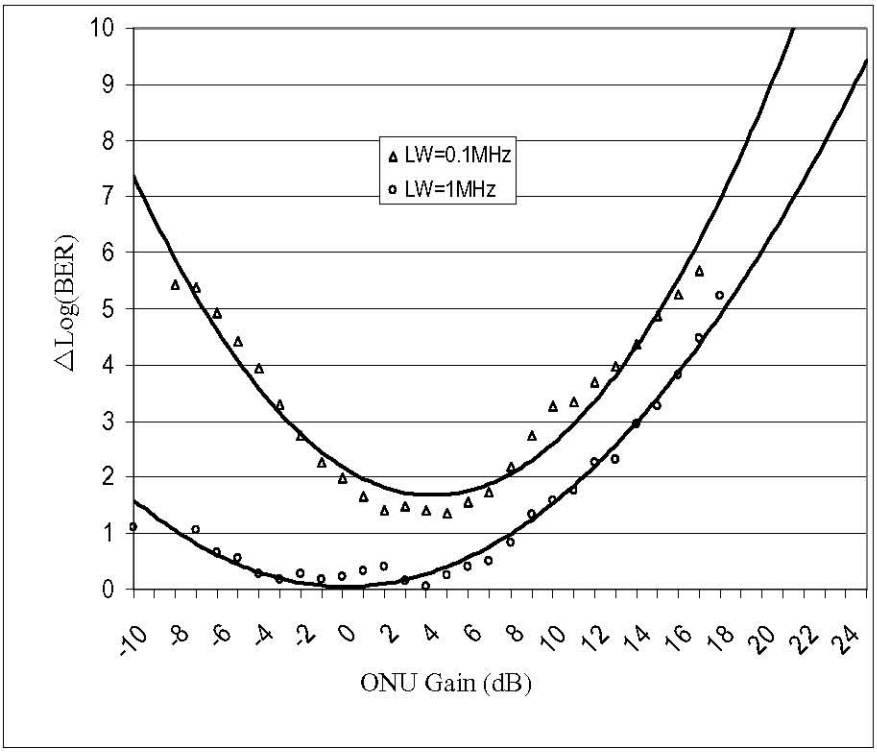

Fig. 4.15 BR penalty in case of different linewidth of the laser source, ORL=30 dB

Chapter 5

Summary and Future Work

In this chapter I summarize the research conducted in this thesis. I also provide possible future work.

5.1 Summary

- In chapter 2 I discussed various techniques that can be used in PONs, and argued that WDM-PONs present an ultimate solution for the continuously increasing demand of bandwidth. I explained how one of the main issues in WDM-PONs is their high cost coming from the need for a separate laser source that is customized for each end user. I then discussed several solutions for the high cost laser source at the ONU, and showed that by using the same downstream signal for upstream, remodulation scheme is a promising solution for implementing source-free ONU, and it solves both the problems of laser sources inventory and the high cost of laser source at the user side.

- In chapter 3 I discussed the importance of phase modulation in optical communication systems, and explained that DPSK offers several advantages on OOK such as the improved receiver sensitivity of 3dB which helps in extending the transmission distance. I gave an overview of the basic devices used in DPSK, and emphasized the direct detection technique given its lower cost and less complexity when compared with the coherent one. I also covered the main impairment that signals suffer in bidirectional systems, and focused mainly on CD and BR beat noise.

- In chapter 4 I proposed a novel WDM-PON scheme that uses both the advantages of DPSK and wavelength remodulation. The system employed NRZ-DPSK for downstream and RZ-DPSK for upstream. The simple yet efficient design of the system is based on removing downstream data form downstream signal using a pulse carver at the ONU, and then remodulating the light for upstream transmission.

  The proposed system was experimentally demonstrated, and it was operated error-free after down and upstream transmission along a bidirectional 20-Km SMF without dispersion compensation.

  I showed the detailed setup and the principle of operation, in addition to the experimental results. When compared with other remodulation schemes, the proposed system showed an enhanced tolerance toward CD, and a penalty of around 4dB coming from BR.

- The novel system that I designed led me to explore the BR penalty when using phase modulation in remodulated WDM-PONs, an issue that is investigated for the first time. Therefore I implemented a setup to analyze the penalty of BR and demonstrated how it is directly related to the gain of the ONU, and depicted how it also depends on the ORL, the TLL, and emphasized the role of the destructive port of the DLI in suppressing BR I signals relative to their bandwidth.

  I found that there is an optimum ONU gain at which the BR penalty is minimized. These results can be significant when designing a remodulation system with phase modulation by tuning the ONU gain to realize the least possible BR penalty.

  Based on my experimental results I argued that BR can not be isolated from dispersion by using a method of separating downstream from upstream then using bidirectional fiber and comparing the two cases, but other methods of comparison need to be used such as using DSF or dispersion compensation, because in the case of using bidirectional transmission dispersion will not only affect the transmitted signals but also the backreflected signals.

5.2 Future Work

- One of the most important sources of noise on upstream signals in remodulation systems is the downstream data itself, and the performance of the system depends on the quality of downstream data removal which in turn depends on the removal technique.

  In my proposed remodulation scheme, the most significant feature is the high efficiency in removing downstream data from the optical carrier in the ONU, and the removal technique that I used can be applied to several other modulation formats.

  Given the importance of spectral efficiency in WDM-PONs, and the significant improvement that Differential Quadrature Phase Shift Keying (DQPSK) offers in this field, using DQPSK in the same system can be investigated for both downstream and upstream as a future work.

- In addition, BR penalty in WDM-PONs remodulation systems could be further investigated with other advanced modulation formats like DQPSK, 8-DPSK, and 16 QAM (Quadrature Amplitude Modulation). A theoretical model of BR penalty that applies to advanced modulation formats can be developed, and any experimental results could be then compared to that of the model.

References:

[1] G. Maier, M. Martinelli, A. Pattavina, and E. Salvadori. Design and cost performance of the multistage wdm-pon access networks. IEEE/OSA Journal of Lightwave Technology, 18(2):125—143, February 2000.

[2] P.-J. Rigole, S. Nilsson, L. Backbom, T. Klinga, J. Wallin, B. Stalnacke, E. Berglind, and B. Stoltz. Access to 20 evenly distributed wavelengths over 100 nm using only a. single current tuning in a four-electrode monolithic semiconductor laser. IEEE Photonics Technology Letters, 7(11):1249—1251, November 1995.

[3] Shiyu Gao, Hanwu Hu, and Hanan Anis, "Impact of Backreflections on Single-Fiber Bidirectional Transmission in WDM-PONs," J. Opt. Commun. Netw. 3, 797-805 (2011)

[4] S. S. Wagner and T. E. Chapuran. Broadband high-density wdm transmission using superluminescent diodes. IEEE Electronics Letters, 26(11):696—697, May 1990.

[5] D.J. Shin, Y. C. Keh, J. W. Kwon, E. H. Lee, J. K. Lee, M. K. Park, J. W. Park, Y. K. Oh, S. W. Kim, I. K. Yun, H. C. Shin, D. Heo, J. S. Lee, H. S. Shin, H. S. Kim, S. B. Park, D. K. Jung, S. Hwang, Y. J. Oh, D. H. Jang, and C. S. Shim. Low-cost wdm-pon with colorless bidirectional transceivers. IEEE/OSA Journal of Lightwave Technology, 24(1):158—165, January 2006.

[6] D. K. Jung, H. Kim, K. H. Han, and Y. C. Chung. Spectrum-sliced bidirectional passive optical network for simultaneous transmission of wdm and digital broadcast video signals. IEEE Electronics Letters, 37(5):308—309, March 2001.

[7] M.H. Reeve, A. R. Hunwicks, W. Zhao, S.G. Methley, L. Bickers, and S. Hornung. Led spectral slicing for single-mode local loop applications. IEEE Electronics Letters, 24(7):389—390, March 1988.

[8] M. Zirngibl, C. H. Joyner, L. W. Stulz, C. Dragone, H. M. Presby, and I. P. Kaminow. Larnet, a local access router network. IEEE Photonics Technology Letters, 7(2):215— 217, February 1995.

[9] R.D. Feldman. Crosstalk and loss in wavelength division multiplexed systems employing spectral slicing. IEEE/OSA Journal of Lightwave Technology, 15(10):1823—1831, October 1997.

[10] H. D. Kim, S.-G. Kang, and C.-H. Le, A low-cost WDM source with an ASE injected Fabry–Perot semiconductor laser, IEEE Photon. Technol. Lett., vol. 12, no. 8, Aug. 2000, pp. 1067–1069.

[11] S.-M. Lee, K.-M. Choi, S.-G. Mun, J.-H. Moon, and C.-H. Lee. Dense wdm-pon based on wavelength-locked fabry-perot laser diodes. IEEE Photonics Technology Letters, 17(7):1579—1581, July 2005.

[12] L. Y. Chan, C. K. Chan, D. T. K. Tong, F. Tong, and L. K. Chen. Upstream traffic transmitter using injection-locked fabry-perot laser diode as modulator for wdm access networks. IEEE Electronics Letters, 38(1):43-45, January 2002.

[13] F.-T. An, K. S. Kim, Y.-L. Hsueh, M. Rogge, W.-T. Shaw, and L. G. Kazovsky. Evolution, challenges and enabling technologies for future wdm-based optical access networks (invited paper). In Joint Conference on Information Systems JCIS 2005', pages 1449-1453, September 2003.

[14] S. L. Woodward, P. P. Reichmann, and N. C. Frigo. A spectrally sliced pon employing fabry-perot lasers. IEEE Photonics Technology Letters, 10(9):1337—1339, September 1998.

[15] C. Arellano, C. Bock, J. Prat, and K.-D. Langer. Rsoa-based optical network units for wdm-pon. In Optical Fiber Communication Conference OFC 2006, March 2006.

[16] N. J. Frigo, P. P. Iannone, P. D. Magill, T. E. Darcie, M. M. Downs, B. N. Desai, U. Koren, T. L. Koch, C. Dragone, H. M. Presby, and G. E. Bodeep. A wavelength-division multiplexed passive optical network with cost-shared components. IEEE Photonics Technology Letters, 6(11):1365—1367, November 1994.

[17] J. Kani, M. Teshima, K. Akimoto, N. Takachio, H. Suzuki, K. Iwatsuki, and M. Ishii. A wdm-based optical access network for wide-area gigabit access services. IEEE Communications Magazine, 41(2):S43—S48, February 2003.

[18] H. Takesue and T. Sugie. Wavelength channel data rewrite using saturated soa modulator for wdm networks with centralized light sources. IEEE/OSA Journal of Lightwave Technology, 21(11):2546—2556, November 2003.

[19] CIP Photonics Press Release. Ground breaking technology deployed by consortium to enable uncooled operation of advanced photonic devices, February 2006.

[20] Proakis, J . G. (2000). Digital Communications. McGraw Hill, New York, fourth edition.

[21] Betti, S., de Marchis, G., and Iannone, E. (1995). Coherent Optical Communication Systems. John Wiley & Sons, New York.

[22] Goodwin, F. E. (1967). A 3.39-micron infrared optical heterodyne communication system. IEEE J. Quantum Electron., QE3(11):524-531.

[23] Chan, V. W. S. (2003). Optical satellite networks. J. Lightwave Technol., 21(11):2811 2827.

[24] Kazovsky, L. G. (1989). Phase- and polarization-diversity coherent optical techniques. J. Lightwave Technol., 7(2):279-292.

[25] Henry, P. S. and Personick, S. D., editors (1990). Coherent Lightwave Communications. IEEE Press, New York.

[26] Shimada, S., editor (1995). Coherent Lightwave Communications Technology. Kluwer Academic, Dordrecht, The Netherlands.

[27] Desurvire, E., Simpson, J. R., and Becker, P. C. (1987). High gain Erbium-doped traveling wave fiber amplifier. Opt. Lett., 12(11):888-890.

[28] Griffin, R. A. and Carter, A. C. (2002). Optical differential quadrature phase-shift key (oDQPSK) for high capacity optical transmission. In Optical Fiber Commun. Conf., paper WX6.

[29] Abbas, G.; Chan, V.; Ting Yee; , "A dual-detector optical heterodyne receiver for local oscillator noise suppression," Lightwave Technology, Journal of , vol.3, no.5, pp.1110-1122, October 1985 doi: 10.1109/JLT.1985.1074301

[30] Tonguz, 0. K. and Wagner, R. E. (1991). Equivalence between preamplified direct detection and heterodyne receivers. IEEE Photon. Technol. Lett., 3(9):835837.

[31] Gnauck, A. H., Reichmann, K. C., Kahn, J. M., Korotky, S. K., Veselka, J. J., and Koch, T.L. (1990). bGb/s heterodyne transmission experiments using ASK, FSK and DPSK modulation. IEEE Photon. Technol. Lett., 2(12):908--910.

[32] Keang-Po Ho., "Phase-modulated optical communication systems, p.36, Springer.

[33] A. H. Gnauck and P. J. Winzer, "Optical phase-shift-keyed transmission," J. Lightw. Technol., vol. 23, no. 1, pp. 115–130, Jan. 2005.

[34] P. J. Winzer, C. Dorrer, R.-J. Essiambre, and I. Kang, "Chirped return- to-zero modulation by imbalanced pulse carver driving signals", IEEE Photon. Technol. Lett., vol. 16, pp. 1379–1381, 2004.

[35] Hwan Seok Chung; Sun Hyok Chang; Kwangjoon Kim; , "Mitigation of Imperfect Carver-Induced Phase Distortions in a Coherent PM-RZ-QPSK Receiver," Lightwave Technology, Journal of , vol.28, no.24, pp.3506-3511, Dec.15, 2010

[36] Wang, J. and Kahn, J. M. (2004b). Impact of chromatic and polarization-mode dispersions on DPSK systems using interferometric demodulation and direct detection. J. Lightwave Technol., 22(2):362--371.

[37] T.-K. Chiang, N. Kagi, T. K. Fong, M. E. Marhic, and L. G. Kazovsky, "Cross-phase modulation in dispersive fibers: Theoretical and experimental investigation of the impact of modulation frequency," IEEE Photon. Technol. Lett., vol. 6, pp. 733–735, June 1994.

[38] M. Fujiwara, J. I. Kani, H. Suzuki, and K. Iwatsuki, "Impact of backreflection on upstream transmission in WDM single-fiber loopback access networks," IEEE J. Lightwave Technol., vol. 24, no. 2, pp. 740- 746, Feb. 2006.

[39] V. O'Byrne. Verizon's fiber to the premises: Lessons learned. In Optical Fiber Communication Conference OF C 2005, March 2005.

[40] M. Feuer, M. Thomas, and L. Lunardi, "Backreflection and loss in singlefiber loopback networks," IEEE Photon. Technol. Lett., vol. 12, no. 8, pp. 1106–1108, Aug. 2000.

[41] N. Buldawoo, S. Mottet, H. Dupont, D. Sigogne, and D. Meichenin, "Transmission experiment using a laser amplifier-reflector for DWDM access network," in Proc. Eur. Conf. Optical Communication (ECOC), Madrid, Spain, 1998, vol. 1, pp. 273–274. Madrid, Spain, 1998, vol. 1, pp. 273–274.

[42] H. Hu and H. Anis, "Degradation of bi-directional single fiber transmission in WDM-PON due to beat noise," IEEE J. Lightwave Technol., vol. 26, no. 8, pp. 870-881, April 2008.

[43] I. Kaminow, T. Li, and A. Willner, eds., Optical Fiber Telecommunications V B: Systems and Networks (Elsevier, 2008), page 278.

[44] L. Y. Chan, C. K. Chan, D. T. K. Tong, F. Tong, and L. K. Chen, "Upstream traffic transmitter using injectionlocked Fabry–Perot laser diode as modulator for WDM access networks," Electron. Lett. 38(1), 43–45 (2002).

[45] J. Zhao, L. K. Chen, and C. K. Chan, "A novel re-modulation scheme to achieve colorless high-speed WDMPON with enhanced tolerance to chromatic dispersion and re-modulation misalignment," in Proc. OFC, Anaheim, CA, Mar. 25–29, 2007, Paper OWD2.

[46] W. Hung, C. K. Chan, L. K. Chen, and F. Tong, "An optical network unit for WDM access networks with downstream DPSK and upstream remodulated OOK data using injection-locked FP laser," IEEE Photon. Technol. Lett. 15(10), 1476–1478 (2003).

[47] J. Xu and L. K. Chen, "Optical Phase Remodulation for 10-Gb/s WDM-PON with Enhanced Tolerance to Rayleigh Noise", OFC/NFOEC 2010, paper OThG3, San Diego.

[48] J. Xu and L. K. Chen, "A New Remodulation Scheme for WDM-PONs With Enhanced Tolerance to Chromatic Dispersion and Remodulation Misalignment," IEEE Photon. Technol. Lett. 22(7), 456–458 (2010).

[49] A. H. Gnauck and P. J. Winzer, "Optical phase-shift-keyed transmission," J. Lightwave Technol. 23(1), 115–130 (2005).

[50] J. Xu, L. K. Chen, and C. K. Chan, "High Extinction Ratio Phase Re-modulation for 10-Gb/s WDM-PON with Enhanced Tolerance to Rayleigh Noise, " International Conference on Optical Internet, COIN 2010, Paper P1061, Korea, Jeju, Jul. 2010.

[51] Nebras Deb and Hanan Anis, "Wavelength remodulation scheme using DPSK downstream and upstream for DWDM-PONs," Opt. Express 19, 16418-16422 (2011)

[52] Jing Xu; Lian-Kuan Chen; Chun-Kit Chan; , "Phase-Modulation-Based Loopback Scheme for Rayleigh Noise Suppression in 10-Gb/s Carrier-Distributed WDM-PONs," Photonics Technology Letters, IEEE , vol.22, no.18, pp.1343-1345, Sept.15, 2010

[53] Jing Xu, Ming Li, and Lian-Kuan Chen, "Rayleigh Noise Reduction in 10-Gb/s Carrier-Distributed WDM-PONs Using In-Band Optical Filtering," J. Lightwave Technol. 29, 3632-3639 (2011)